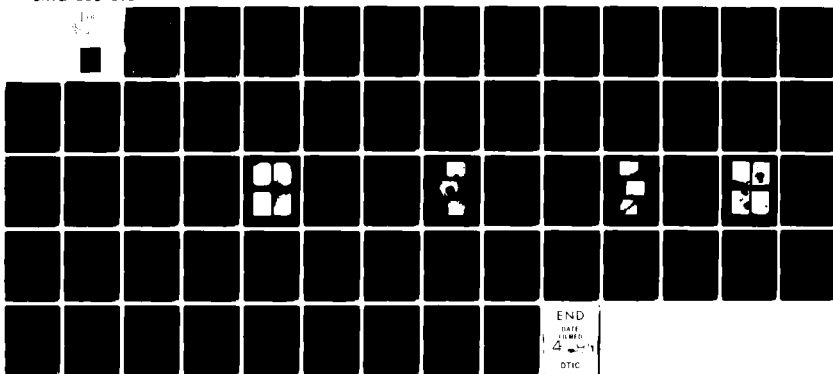
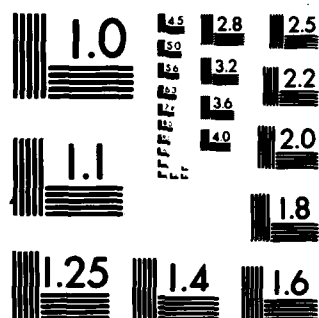


AD-A096 260 MASSACHUSETTS INST OF TECH CAMBRIDGE DEPT OF CHEMICA--ETC F/G 11/9  
MORPHOLOGY AND MECHANICAL BEHAVIOR OF BLENDS AND DIBLOCK COPOLY--ETC(U)  
FEB 81 R E COHEN, D E WILFONG N00014-77-C-0311  
UNCLASSIFIED TR-7 NL





MICROCOPY RESOLUTION TEST CHART  
NATIONAL BUREAU OF STANDARDS-1963-A

AD A 096260

OFFICE OF NAVAL RESEARCH

Contract <sup>15</sup> N00014-77-C-0311

Task No. NR 356-646

<sup>12</sup>  
yw  
**LEVEL II**

<sup>1</sup> Technical Report No. 7

<sup>6</sup> Morphology and Mechanical Behavior of Blends  
and Diblock Copolymers of 1,2 and 1,4 Polybutadiene.

<sup>12</sup> 63

by

<sup>14</sup> <sup>10</sup> Robert E. Cohen and David E. Wilfong

Department of Chemical Engineering  
Massachusetts Institute of Technology  
Cambridge, Massachusetts 02139

DTIC  
MAR 12 1981

E

<sup>11/25</sup> Feb 21  
February 25, 1981

Reproduction in whole or in part is permitted  
for any purpose of the United States Government

This document has been approved for public release and sale:  
its distribution is unlimited

FILE COPY

220005

81 3 11 001

JLB

REPORT DOCUMENTATION PAGE		READ INSTRUCTIONS BEFORE COMPLETING FORM
1. REPORT NUMBER	2. GOVT ACCESSION NO <b>AD-A096260</b>	3. RECIPIENT'S CATALOG NUMBER
4. TITLE (and Subtitle) <b>Morphology and Mechanical Behavior of Blends and Diblock Copolymers of 1,2 and 1,4 Polybutadiene</b>		5. TYPE OF REPORT & PERIOD COVERED <b>Technical Report</b>
7. AUTHOR(s) <b>R.E. Cohen, D.E. Wilfong</b>		6. PERFORMING ORG. REPORT NUMBER <b>7</b> ✓
9. PERFORMING ORGANIZATION NAME AND ADDRESS <b>Department of Chemical Engineering Massachusetts Institute of Technology Cambridge, MA 02139</b>		8. CONTRACT OR GRANT NUMBER(s) <b>N00014-77-C-0311</b> ✓
11. CONTROLLING OFFICE NAME AND ADDRESS <b>Office of Naval Research 800 N. Quincy Street Arlington, VA 22217</b>		10. PROGRAM ELEMENT, PROJECT, TASK AREA & WORK UNIT NUMBERS <b>NR-356-646</b>
14. MONITORING AGENCY NAME & ADDRESS (if different from Controlling Office)		12. REPORT DATE <b>February 25, 1981</b>
		13. NUMBER OF PAGES <b>55</b>
		15. SECURITY CLASS. (of this report)
		15a. DECLASSIFICATION/DOWNGRADING SCHEDULE
16. DISTRIBUTION STATEMENT (of this Report)		
17. DISTRIBUTION STATEMENT (of the abstract entered in Block 20, if different from Report)		
18. SUPPLEMENTARY NOTES		
19. KEY WORDS (Continue on reverse side if necessary and identify by block number) <b>elastomers, polydiene microstructure, viscoelastic properties, homogeneous block copolymers, heterogeneous block copolymers, morphological transitions</b>		
20. ABSTRACT (Continue on reverse side if necessary and identify by block number) <b>The structure and mechanical properties of a series of polymer blends and block copolymers comprised of medium cis 1,4-polybutadiene and 99% 1,2-polybutadiene have been investigated. Thermal properties (DSC) were determined at two levels of radiation crosslinking and for various sample preparation procedures (solvent and thermal history). Dynamic mechanical spectra (3.5 Hz) were measured over temperature range from 180 to 310K. Transmission electron microscopy was also used for establishing the number phases and the domain size and geometry in the heterogeneous materials.</b>		

Stress-strain curves were determined for the various samples as a function of crosslink density and casting solvent. Equilibrium swelling ratios were measured for each specimen at the same radiation dose in a good solvent. Swelling values were also obtained in a series of solvents for the parent homopolymers and for a diblock copolymer containing 45% 1,2 polybutadiene.

Results indicate the homopolymer blends were heterogeneous, containing 1-50 micron size spherical inclusions of the minor component. The 45% 1,2-diblock sample exhibited lamellar microdomains 20 to 30 nm in width while the remaining diblock samples of lower 1,2- content and higher overall molecular weight appeared homogeneous. Morphological results are discussed in relation to current thermodynamic theories of diblock phase separation.

## INTRODUCTION

This report presents results obtained on a novel set of rubbery-rubbery diblock copolymers. Each diblock contain one segment of the well known an-ionically polymerized 1,4 polybutadiene (microstructure: 35% cis 1,4; 51% trans 1,4; 13% 1,2) and one segment consisting of essentially pure 1,2 polybutadiene, a microstructure only recently reported (1,2) in the literature. Results are also presented on various polymer blends comprised of various proportions of two homopolymers with microstructures identical to those described above.

Unlike the previously investigated diblock copolymers of 1,4 polybutadiene and cis 1,4 polyisoprene which were homogeneous in all proportions (3-6), the diblocks under investigation here are either homogeneous or heterogeneous depending upon overall molecular weight and composition. In the report, attempts are made to compare in a qualitative manner our information on this homogeneous to heterogeneous transition with recent theoretical studies of phenomenon. The rubbery-rubbery nature of our samples is seen as a major advantage in obtaining samples which are close to equilibrium at room temperature, a condition which facilitates comparisons with the thermodynamic theories. Continued work on these polymers is aimed at obtaining appropriate parameters to allow for a more quantitative comparison with theory.

Accession For	
NTIS GR&I	<input checked="" type="checkbox"/>
DTIC TAB	<input type="checkbox"/>
Unannounced	<input type="checkbox"/>
Justification	
By _____	
Distribution /	
Availability Codes	
Dist	Special
A	

## Materials and Experimental Procedures

### Materials

#### . Origin

The polymer sample series used in this study was obtained from Dr. Adel F. Halasa of Firestone Tire and Rubber Company. Synthesis details for the homopolymers and diblocks were also made available by Dr. Halasa ( 1. 2 ).

#### Synthesis

The 1,2- polybutadiene homopolymer was prepared via anionic polymerization of 1,3- butadiene monomer in n- hexane using n- butyllithium as an initiator in the presence of dipiperidene ethane, DPE (  $(\text{HN}-\text{C}_5\text{H}_9)-\text{CH}_2\text{CH}_2-(\text{C}_5\text{H}_9\text{NH})$  ). Addition of this polar modifying agent ( $\text{Li/DPE} = 4.0$ ) to the reaction medium resulted in a polybutadiene microstructure of 99% 1,2-. The corresponding 1,4 homopolymer was synthesized by excluding DPE from the procedure, yielding a 35% cis 1,4; 51% trans 1,4; and 13% 1,2- PBD microstructure. The diblocks were made by the sequential addition of fresh 1,3- butadiene monomer and DPE to non-terminated polybutadienyl lithium chains which had been polymerized without the modifier. The molecular weight of both blocks was controlled by the concentration of n- butyllithium initiator and the amount of fresh monomer added in the second block synthesis. Termination of all polybutadienyl lithium anions occurred during precipitation of the polymer in a proton donating solvent such as methanol.

### Sample Preparation

#### Cleaning

The polymer samples as received from Firestone were heavily loaded with anti-oxidant to inhibit possible degradation of these highly conjugated materials. This was

apparent from the various red to brown colors exhibited by the samples which are colorless when pure. To remove these and other impurities (particulates possibly from post-synthesis processing), the polymers were dissolved in technical grade toluene (Package Chemical Company, Inc., Boston, MA 02127), decanted to remove insolubles, and then extracted in methanol (Package Chemical Company, Inc., Boston, MA 02127). The white precipitate was vacuum dried for a minimum of 2 days and then stored under nitrogen at 250K until further use.

#### Film Casting

Thin films with uniform thickness suitable for mechanical testing were prepared by solution casting. Solutions of 5% polymer by weight were made by dissolving cleaned polymer in a selected solvent, avoiding exposure to light, oxygen, and mechanical agitation. Polymer blends were made by simply dissolving predetermined amounts of each homopolymer to form a 5% casting solution. Solvent evaporation was done using the spin casting technique of Kaelble (7) at room temperature. A schematic view of the apparatus used is shown in Figure 1. It consists of a removable aluminum casting cup mounted on a vertically positioned motor shaft. During operation, the motor rotates at 3450 rpm, generating a centripetal acceleration of  $\sim 600g$  at the cup's inner wall. The polymer solution is added to the spinning cup through a hole in the cup lid. As the solvent evaporates, a film with outstanding thickness uniformity is deposited on teflon film lining the cup walls, which can be easily removed when casting is complete.  $N_2(g)$  is injected at  $1.5 \times 10^{-3} \text{ liters} \cdot \text{sec}^{-1}$  through the hole in the cover lid to minimize the flow of dust and air into the cup and also to facilitate solvent removal. Films cast from cyclohexane were removed after 24 hours and those cast from toluene after 48 hours.



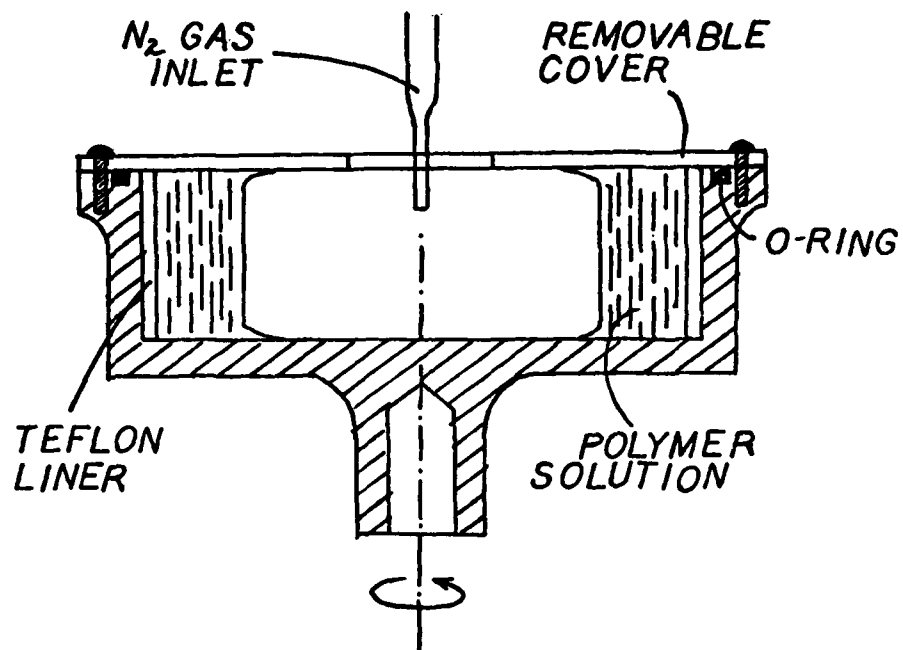


Figure 1: Sample spin casting cup.

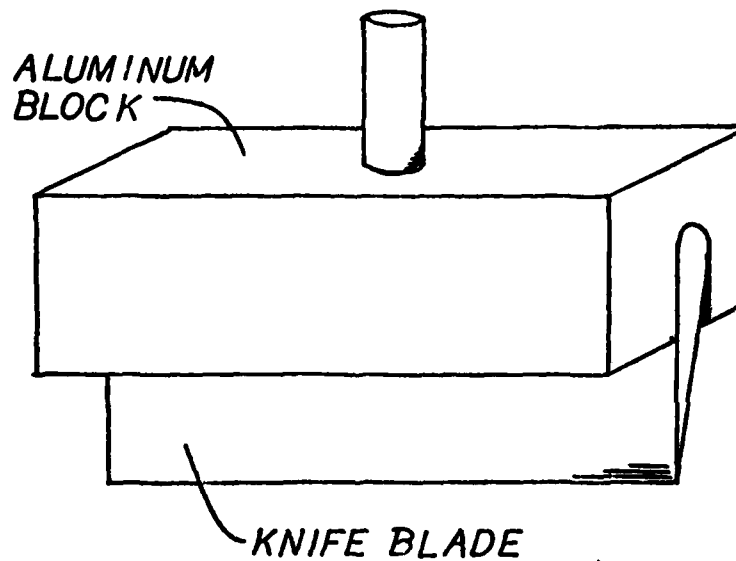


Figure 2: Tensile and dynamic mechanical test sample cutter.

Upon removal from the casting cup, the sample films and liner were tacked down and dried for one day under nitrogen at 0.6 atm and ambient temperature. This was followed by 48 hours at full vacuum before the film was ready for use. Samples not immediately processed after the two days of vacuum drying were stored under vacuum at room temperature and protected from light.

#### Crosslinking

With the exception of a few samples used in the thermal analysis, all films were crosslinked to provide suitable materials for mechanical testing and swelling studies. Crosslinking was achieved by irradiating the films on their teflon liners in air using a Van de Graaft electron accelerator (8). The films were exposed to a 3MeV electron beam on a conveyor belt with a dose of 1.7 to 2.5MRad per pass. Total doses of 2,4,10, and 30MRad were obtained. A stream of air was blown over the films during this process to minimize heat build-up.

#### Cutting

All samples used in mechanical and dynamic mechanical testing were cut using a microtome knife blade (American Optical Inc.) mounted in an aluminum block shown in Figure 2. This assembly is placed in the chuck of a drill press. Samples are clamped to the movable platen allowing uniform test strips to be cut. Samples which were not immediately tested were stored under full vacuum at ambient temperature and protected from light.

#### Experimental Techniques

##### H<sup>1</sup> - NMR

A 60MHz EM360 Varian Nuclear Magnetic Resonance Spectrometer was used to record the spectra of 5% polymer solutions in benzene. Tetramethylsilane (TMS) was included in

each solution as an internal standard. All runs were performed at room temperature.

#### High Performance Size Exclusion Chromatography (HPSEC)

All polymer samples were tested on DuPont Zorbax PSM Bimodal-s columns (DuPont Company, Scientific & Process Instruments Division, Wilmington, DE) with a mobile phase of THF and a flow rate of  $1.67 \times 10^{-5}$  liter $\cdot$ sec $^{-1}$  at 298K. Monodisperse polystyrene samples were used to construct a universal calibration curve. Final values of molecular weight were determined using the method of Prudhomme (9) for calculating diblock molecular weights and tabulated Mark-Houwink parameters.

#### Differential Scanning Calorimetry

The glass transition temperature of each polymer was measured using a Perkin-Elmer DSC-II Differential Scanning Calorimeter equipped with an Auto Scanning Zero. Thermograms were obtained in the heating mode on  $1.5$ - $3.0 \times 10^{-2}$  g samples. These were quenched from room temperature to 150K at  $5.33^{\circ}$ .sec $^{-1}$  and heated to 300K at  $0.33^{\circ}$ .sec $^{-1}$ . Liquid nitrogen was used as a system coolant and argon gas as a purge for the cooling chamber. Benzoic acid and indium were used to calibrate the instrument.

#### Instron Testing

Stress-strain measurements on  $0.65\text{mm} \times 6.5\text{mm} \times 90\text{mm}$  tensile strip specimens (crosslinked and cut as previously described) were taken on a 1122 Instron Tensile Tester equipped with a 2000g load cell at  $298 \pm 2\text{K}$ . Elongation rates of  $1.67 \times 10^{-4}$  and  $1.67 \times 10^{-3}$  m $\cdot$ sec $^{-1}$  were used. Load and displacement data were reduced

to true stress (MPa), assuming constant volume, and % elongation. All reported data are based on an average of five different runs.

### Rheovibron

All dynamic tensile data were obtained on a Rheovibron model DDV-II-C Direct Reading Viscoelastomer (Toyo Baldwin Company, Ltd., Tokyo, Japan) equipped with a Tektronics 502A Dual-beam Oscilloscope (Tektronics, Inc., Portland, OR) and a low temperature chamber (IMASS Inc., Accord, MA). Samples crosslinked with 2 and 30 MRad electron doses were tested over approximate temperature ranges of  $-100^{\circ}\text{C}$  to  $20^{\circ}\text{C}$  and  $-60^{\circ}\text{C}$  to  $30^{\circ}\text{C}$ , respectively. In order to obtain data over the broad temperature range of the 2 MRad series,

two specimens were needed. The Massa correction (10,11) was applied to correct for the use of specimens of differing length to cross sectional area ratios and the instrument compliance.

All runs were done at a frequency of 3.5Hz under a blanket of  $\text{N}_2(\text{g})$ . The heating rate was kept at  $2 \times 10^{-2}^{\circ}\text{C} \cdot \text{sec}^{-1}$  to insure equilibrium. Metal tabs were end-buttet to all samples according to the procedure of Voet (12) thus eliminating the need for a grip correction.

### Electron Microscopy

Variation in electron density between discrete phases in heterogeneous blocks and blends is necessary for resolving morphological features. Because 1,2- and 1,4-polybutadiene are so chemically similar, it was necessary to provide some additional means of contrast. This was accomplished using scattering contrast via the staining technique of Smith and Andries (13) called the ebonite method. This method was chosen over other contrast enhancement techniques because it proved to be successful in contrasting the phases in a heterogeneous blend of high vinyl-(64%) and medium cis- polybutadiene (45% cis, 45%

trans, 10% vinyl)(3,5). The ebonite method involved hardening a 20 x 5 x 0.5mm polymer strip by placing it in a polypropylene vial with a threaded cap, injecting into this a molten sulfur solution at 120°C, and maintaining this temperature using an oil bath for 24 hours. The sulfur solution was composed of sulfur, rubber accelerator (N-t-butyl-2-benzothiazole sulfenamide, R.T. Vanderbilt Co., Inc., Norwalk, CT), and zinc stearate: using a 90:5:5 sulfur/accelerator/stearate weight ratio. This treatment gave a hard, black sample which was suitable for microtoming.

Thin sections of ebonite treated polymer were cut using a LKB Ultratome III microtome (LKB-Produkter AB, Stockholm, Sweden) fitted with a glass knife. Sample thickness varied between 800 and 1400 Å based on their observed interference colors. Glass knives were prepared immediately prior to use via a LKB 7800A Knife Maker (LKB-Produkter AB, Stockholm, Sweden). Cut specimens were floated on water and collected on 200 mesh copper grids (Pelco Products, Ted Pella, Inc., Tustin, CA).

Electron micrographs were obtained using a Philips EM200 electron microscope. Film plate magnification was varied from 1,880 to 94,000x at an accelerating voltage of 80kv. Kodak 4463 electron microscope film was used for photographic reproduction.

#### Swelling

Two separate swelling experiments were performed. The first test was done on homopolymers and diblocks exposed to a 4MRad electron dose. After crosslinking, 0.05g strips of each sample were accurately weighed and swollen in chloroform at room temperature. After two days, the swollen samples were blotted and reweighed in capped weighing bottles. The second experiment was done using polymer samples exposed to a 10MRad electron dose in various solvents. These

0.05g samples were placed in glass containers where they were suspended above the swelling solvent on a copper wire grid, flushed with  $N_2(g)$ , and allowed to swell in the vapor for four days. This technique minimized large solvent concentration gradients at the onset of swelling and eliminated problems with sample cracking. This was followed by an additional four days of swelling in the liquid. Samples were removed from the solvent, swabbed dry, and quickly weighed. After weighing, samples were returned to the liquid phase for a minimum of ten minutes before reweighing to insure no net solvent loss due to evaporation. Evaporative losses were also prevented by judiciously choosing swelling solvents with low vapor pressures. By these methods, the weight loss during weighing was kept below 2% of the total swollen weight. A total of five individual specimens of each sample were weighed a minimum of three times. These three values of initial and final weight for each specimen were then used to calculate a mean initial and final weight. This resulted in five values for the swelling ratio ( $V_f/V_o$ ) whose mean and standard deviation are reported.

## Results and Discussion

### Characterization

A considerable portion of this work was devoted to characterizing the polymer samples supplied by Firestone. This effort can be justified by considering the strong dependence of mechanical and morphological properties of block polymers on the molecular weight of each block, their polydispersity, and the propensity of these parameters to be affected by the environment. Besides the typical problems encountered in anionically synthesizing monodisperse block polymers of known molecular weights (such as deactivation of the initiator, premature chain termination, and chain coupling), diene-diene block polymers possess the additional complication of being highly susceptible to oxidative degradation and crosslinking. Therefore, it is critical that an accurate characterization of the samples be performed prior to mechanical and morphological analyses to insure accurate sample-to-sample comparisons.

Along with the polymer samples, Firestone supplied extensive characterization data which are shown in Table 1. The 1,4- PBD block molecular weight values  $\bar{M}_{n,A}$  were measured by analyzing a small amount of "living" polymer extracted from the reactor prior to the addition of the polar modifier and monomer for the second block. The 1,2- PBD block molecular weights  $\bar{M}_{n,B}$  were calculated using  $\bar{M}_{n,A}$  values, the measured molecular weight values for the final diblocks  $\bar{M}_{n,AB}$ , and the microstructure data on both. The molecular weight values of Firestone shown in Part (a) of Table 1 are in good agreement with those of this lab, shown in Part (b); the primary source of discrepancy was linked to a significant fraction of high molecular

Sample Code	(90/0)	(30/50)	(30/100)	(30/150)	(30/200)	(0/100)
Calculated or Stoichiometric Molecular Wt.						
1,4- Block	-	50K	100K	150K	200K	100K
1,2- Block	90K	30K	30K	30K	30K	-
Part (a)						
1,4- Block						
G.P.C.						
$\bar{M}_n, A$	-	65K	100K	160K	195K	-
$\bar{M}_w/\bar{M}_n$	-	1.08	1.08	1.11	1.11	-
I.R.						
% cis 1,4-	-	34.7	36.2	34.3	37.2	-
% trans 1,4-	-	53.4	52.6	51.1	51.7	-
% 1,2-	-	11.8	11.3	14.6	11.2	-
Total Polymer						
G.P.C.						
$\bar{M}_n, AB$	109K	96K	130K	182K	206K	111K
$\bar{M}_w/\bar{M}_n$	1.08	1.08	1.08	1.11	1.11	1.12
I.R.						
% cis 1,4-	0	22.1	26.4	29.1	32.3	35.1
% trans 1,4-	0.2	32.0	38.7	43.2	44.7	51.8
% 1,2-	99.8	45.9	35.0	27.7	23.1	13.2
1,2- Block						
$\bar{M}_n, B$	-	36.2K	36.9K	26.5K	23.4K	-
Standard deviation, $\sigma$	-	3.7K	6.4K	2.6K	7.8K	-



	(90/0)	(30/50)	(30/100)	(30/150)	(30/200)	(0/100)
Weight Fraction of 1,2- PBD Block	1.00	0.38	0.28	0.15	0.11	0.0
Part (b)						
Total Polymer						
HPSEC						
$\bar{M}_{n,AB}$	85K	83K	133K	165K	202K	97K
$\bar{M}_n$ , IMPURITY	187K	196K	301K	408K	500K	220K
Mole fraction of impurity	0.03	0.06	0.08	0.14	0.15	0.12
Weight Fraction of 1,2- PBD Block (corrected)	-	0.38	0.23	0.17	0.13	-

11

Table 1: Shown in Part (a) are the molecular weight and microstructure data of Firestone. Part (b) shows the results of this lab using HPSEC. The Mark-Houwink parameters for the 1,2- and 1,4- PBD in THF were  $K_{1,2} = 6.13 \times 10^5$ ,  $a_{1,2} = 0.85$  and  $K_{1,4} = 1.56 \times 10^{-4}$ ,  $a_{1,4} = 0.80$ , respectively (as reported by Firestone). The Mark-Houwink constants for the diblocks were calculated using the method of Prud'homme (43).  $\bar{M}_{n,AB}$  values were found from the elution volumes corresponding to the maxima in the SEC traces.

weight impurity being included in their calculated  $\bar{M}_{n,AB}$  values. This impurity, possibly the result of some coupling reaction, was also apparent in our SEC traces (see Figure 3). Its mole fraction  $x$  and molecular weight  $\bar{M}_{n,IMPURITY}$  are included in Part (b) of the table. As a result, the two data sets provide complimentary information: the Firestone values give a good estimate of the polydispersity ( $\bar{M}_w/\bar{M}_n$ ) and microstructure of the various samples while our data provide the best values of molecular weight for each diblock.

The results from the NMR analysis provided a qualitative verification of the reported sample microstructure. Observed chemical shifts for the 1,2- and 1,4- butadiene repeat units were in agreement with those reported by Bovey (14). Samples could be correctly assigned to their corresponding spectra based on relative peak heights.

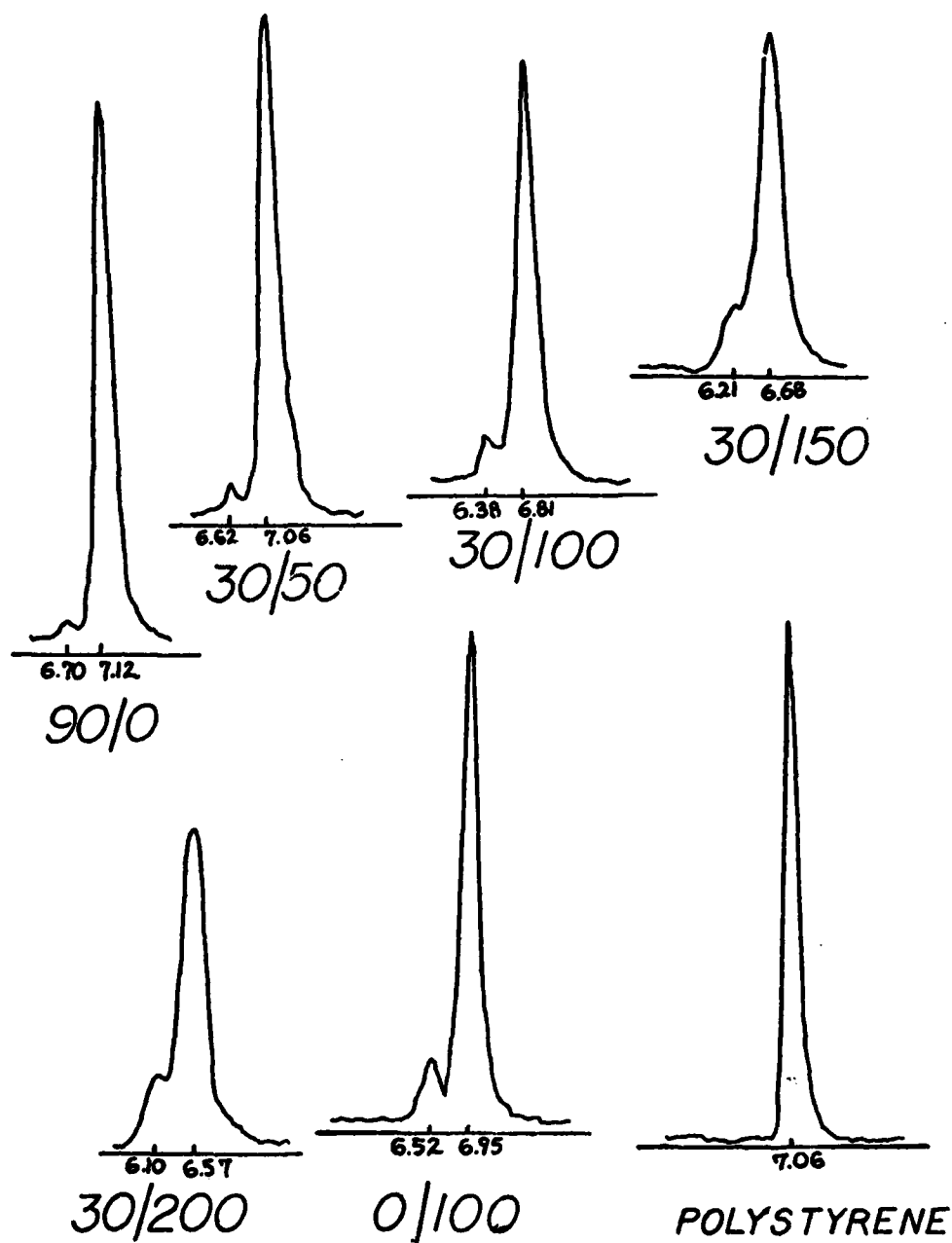


Figure 3 HPSEC elution curves for the 1,2- PBD-b-1,4- PBD diblocks and their corresponding homopolymers. Also shown is a 100K molecular weight polystyrene standard with a known polydispersity of ( $\bar{M}_w/\bar{M}_n$ )= 1.06.

## Thermomechanical Properties

### Thermal Analysis

Glass transition temperatures determined using Differential Scanning Calorimetry for crosslinked and uncrosslinked samples cast from various solvents are shown in Table 2. Values assigned the  $T_{g1}$  and  $T_{g2}$  columns correspond to endotherms observed near the glass transitions of the 1,4- and 1,2- polybutadiene homopolymers, respectively. Also shown are data reported by Firestone (shown in parentheses) and values for certain samples which were lightly crosslinked and then annealed at 350K for two hours under vacuum.

The results from Table 2 show that the casting solvent has no effect on the observed glass transition unlike SBS triblock copolymers which show marked glass transition variations in films cast from various solvents (15). In the SBS triblocks, large chemical dissimilarities between blocks led to strong solvent preferences. In the case of solvent affinity for the butadiene block with a corresponding non-affinity for the polystyrene, regions of virtually pure polystyrene will form first in the casting process. A good solvent for both phases, however, should lead to better mixing of the two components in the cast film since neither would have the same thermodynamic driving force for phase separation along with the corresponding chain mobility available in the more dilute solution for regions of pure component to form. This increase in mixing should vanish when the sample is annealed at a temperature which allows sufficient chain mobility in the melt to result in a thermodynamically stable configuration. In contrast to PS and PBD, the 1,2- and 1,4- blocks are chemically alike and possess similar solubility characteristics,

**PART A****CROSSLINKED SAMPLES (4MRad)**

<u>Sample</u>	<u>Solvent</u>	<u>Annealed <math>\frac{80^{\circ}\text{C}}{2 \text{ hr.}}</math></u>	<u>T<sub>g1</sub>(k)</u>	<u>T<sub>g2</sub>(k)</u>
(30/50)	C <sub>6</sub> H <sub>12</sub>	Yes	191	-
	C <sub>6</sub> H <sub>6</sub>	Yes	191	-
	C <sub>6</sub> H <sub>12</sub>	No	182	-
	Toluene	No	184	-
38% 1,2- PBD blend	C <sub>6</sub> H <sub>6</sub>	Yes	188	278
	C <sub>6</sub> H <sub>12</sub>	Yes	188	278
80% 1,2- PBD blend	C <sub>6</sub> H <sub>12</sub>	Yes	185	274

**PART B****UNCROSSLINKED SAMPLES (Unannealed)**

<u>Sample</u>	<u>Solvent</u>	<u>T<sub>g1</sub>(k)</u>	<u>T<sub>g2</sub>(k)</u>
(90/0)	Toluene	-	271 (271)
(30/50)	Toluene	184 (183)	- (289)
(30/100)	Toluene	186 (182)	-
(30/150)	Toluene	186 (182)	-
(30/200)	Toluene	181 (177)	-
(0/100)	Toluene	179 (178)	-
38% 1,2- PBD blend	C <sub>6</sub> H <sub>12</sub>		280

**Table 2:** DSC results for 1,2- PBD/1,4- PBD diblocks, homopolymers, and homopolymer blends. Values shown in parentheses are those reported by Firestone.

i.e.,  $\delta_{1,2\text{-PBD}} \approx \delta_{1,4\text{-PBD}}$ . Hence, the lack of solvent dependence is a reasonable result.

Radiative crosslinking with an electron dose of 4 MRad resulted in no significant change in  $T_g$  for the (30/50) diblock. Annealing the (30/50) diblock and the 38% 1,2- PBD blend resulted in narrower endotherms for both samples. The observed transitions were also shifted slightly towards the respective homopolymer transitions as shown in Table 2 although annealing never resulted in any distinct transition near that of 1,2- PBD for the (30/50) diblock. The changes in the endotherms for the (30/50) diblock and the 38% 1,2- PBD blend suggest that a significant amount of mixing between phases may exist in the solvent cast samples (16). This is understandable for the same reason that solvent dependence is not expected. A good solvent for 1,2- PBD works equally well for the 1,4- PBD.

Figure 4 shows a plot of glass transition temperature versus percent composition. Included with the data are plots of the Fox equation and the Gordon-Taylor equation (17).

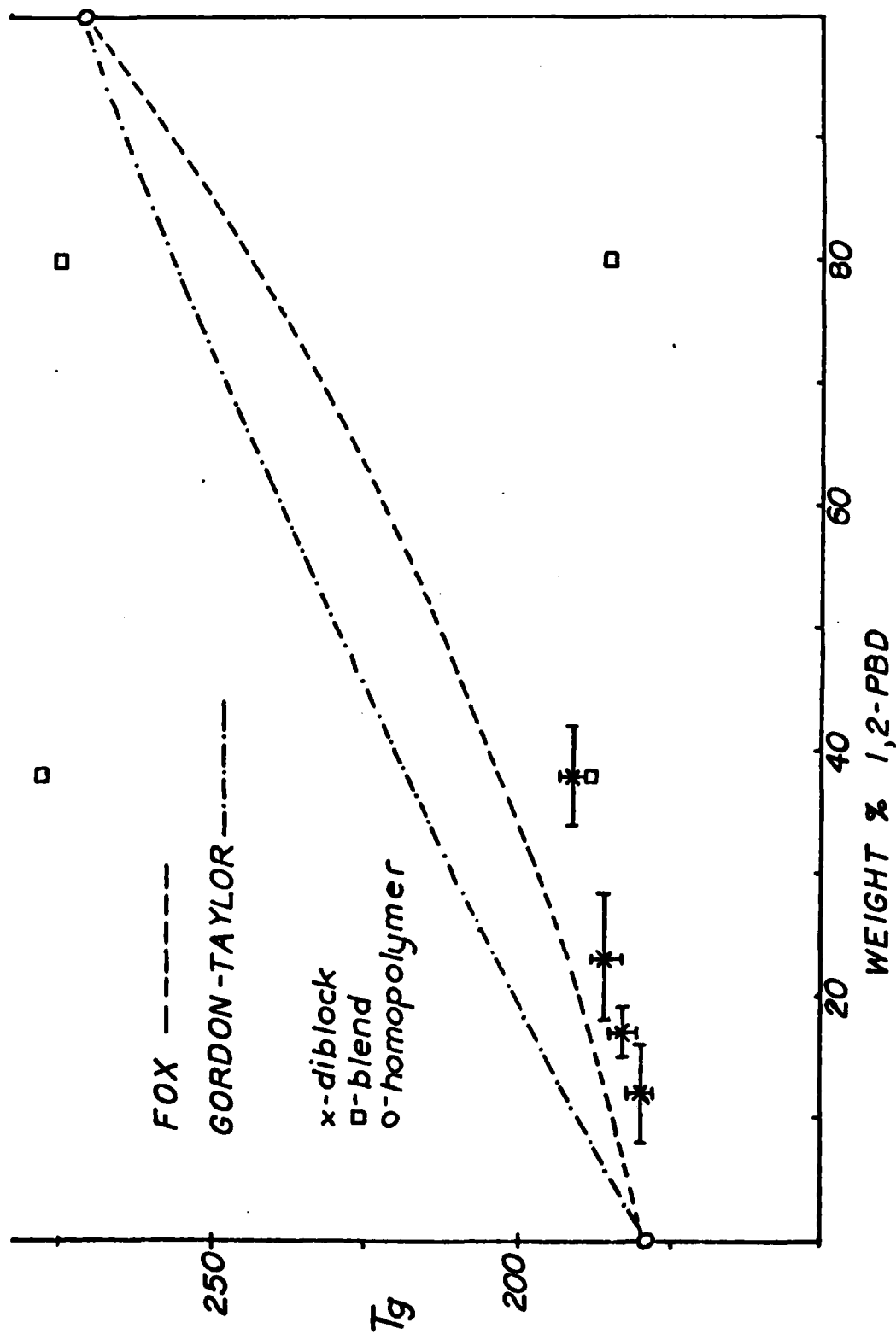


Figure 4: Glass transition temperature vs. composition for 1,2-PBD/1,4-PBD diblocks, homopolymers, and homopolymer blends.

These relationships are commonly used for expressing the composition dependence of  $T_g$  for random copolymers and homogeneous blends.

The data for the 38% and 80% 1,2- PBD blends exhibit two distinct glass transitions and show a strong deviation from the predicted values for miscible systems. These results are indicative of phase separated blends. Each diblock tested, however, failed to show two distinct transitions suggesting sample homogeneity. Unlike the glass transition values for homogeneous diblocks of polyisoprene and polybutadiene which are in excellent agreement with the predicted values of the Gordon-Taylor equation (5), Figure 4 shows that these diblock samples exhibit the same negative deviation from the predicted values as the blends, and suggest that the samples may not be well mixed. This contradiction was experimentally reproducible, thus

thermal analysis of the diblocks gave ambiguous results with regard to sample morphology.

Finally, it was visually apparent that the endotherms for the diblock transitions were generally broader than those for the homopolymers and blends. Because of this and unavoidable baseline deviations in the thermograms,  $T_g$  assignments were sometimes difficult. For this reason, a  $\pm 4^\circ$  error estimate is shown for the diblocks in Figure 4 despite the reported  $2^\circ$  accuracy of the calorimeter.

#### Dynamic Mechanical Properties

The loss tangent  $\tan \delta$  and the tensile storage modulus  $E'$  were measured as a function of temperature for the diblocks, homopolymers, and two homopolymer blends. All of these samples were spin cast from cyclohexane. Rheovibron tests were performed at a frequency of 3.5Hz since previous



studies in this laboratory have shown that better peak resolution in multicomponent systems is obtainable at low frequencies (3-6).

Figure 5 shows  $\log \tan \delta$  and  $\log E'$  plotted versus temperature for the four diblocks and two homopolymer samples crosslinked with a 2Mrad electron dose. The curves for the (30/50) diblock sample coincide with the generalized behavior expected for two phase materials.

The sample exhibits two maxima in  $\log \tan \delta$  near the glass transitions of the two respective homopolymers and the characteristic plateau region in  $\log E'$ . The remaining diblocks show a shift in both  $\log E'$  and  $\tan \delta$  towards higher temperatures. The magnitude of this increase is dependent on the 1,2- PBD content which is reminiscent of the behavior of miscible blends.

Peak broadening in the  $\log \tan \delta$  curves is evident in the diblock samples and also appears to increase with increasing 1,2- PBD content.

The  $\log \tan \delta$  plot also shows a gradual increase in  $\tan \delta$  when  $T > -50^{\circ}\text{C}$  for the (30/100), (30/150), (30,200) and (0/100) samples. Since even the 1,4- homopolymer exhibits this trend of steadily increasing  $\tan \delta$  values with increasing temperature, some mechanism other than a glass transition must be responsible. This additional source of mechanical loss could mask any subtle 1,2- PBD transitions near  $0^{\circ}\text{C}$ . To eliminate the problem of poor resolution in the vicinity of  $0^{\circ}\text{C}$ , dynamic mechanical properties were also measured on more heavily crosslinked samples. The results of these tests for samples exposed to 30Mrad electron doses are shown in Figure 6. The greater crosslink densities resulted in a general broadening of the  $\tan \delta$  peaks. Similar results obtained by others (18) have been attributed to a broader distribution in molecular weight

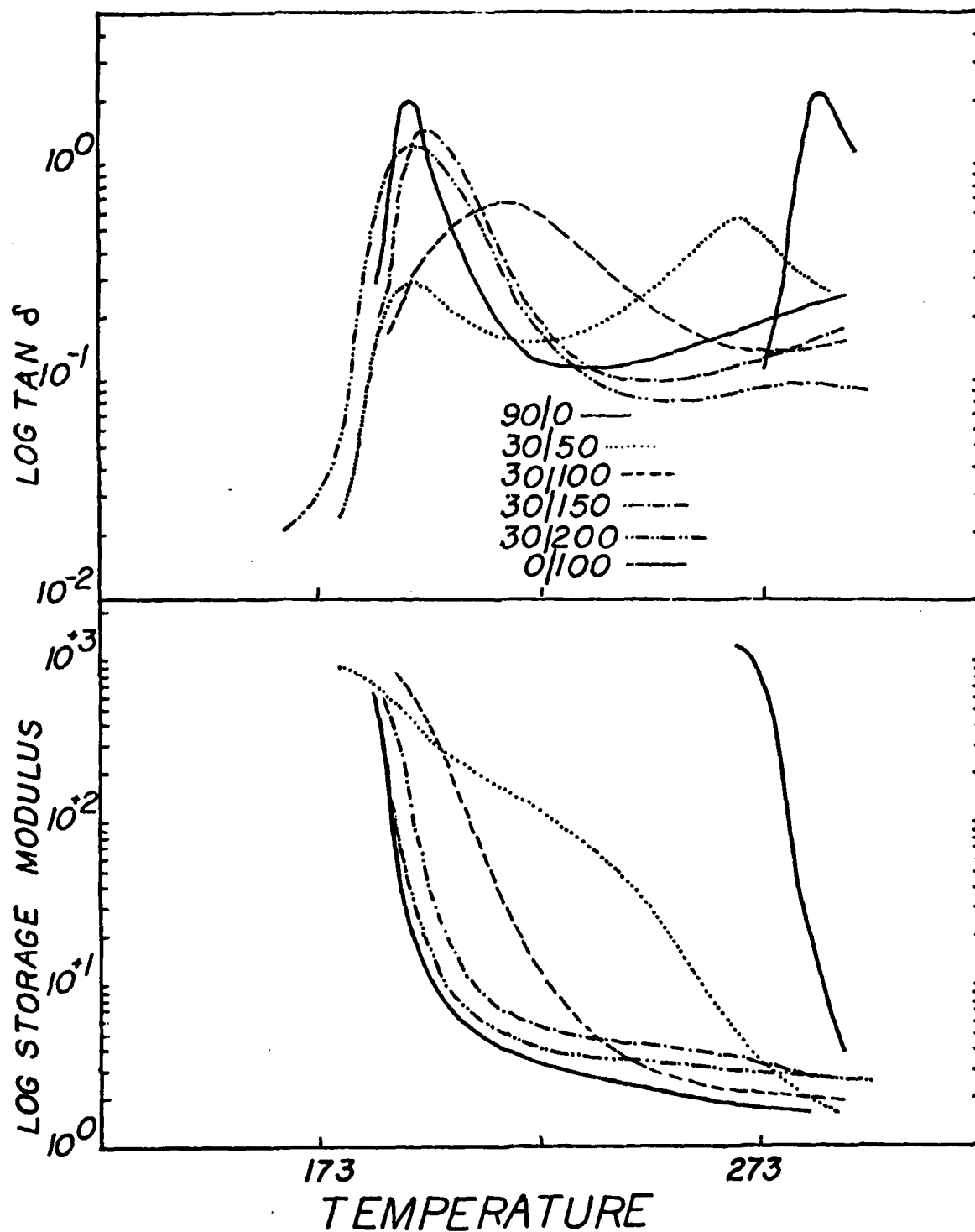


Figure 5 : Dynamic mechanical properties for the diblocks and homopolymers previously treated with a 2MRad electron dose at 3.5Hz.

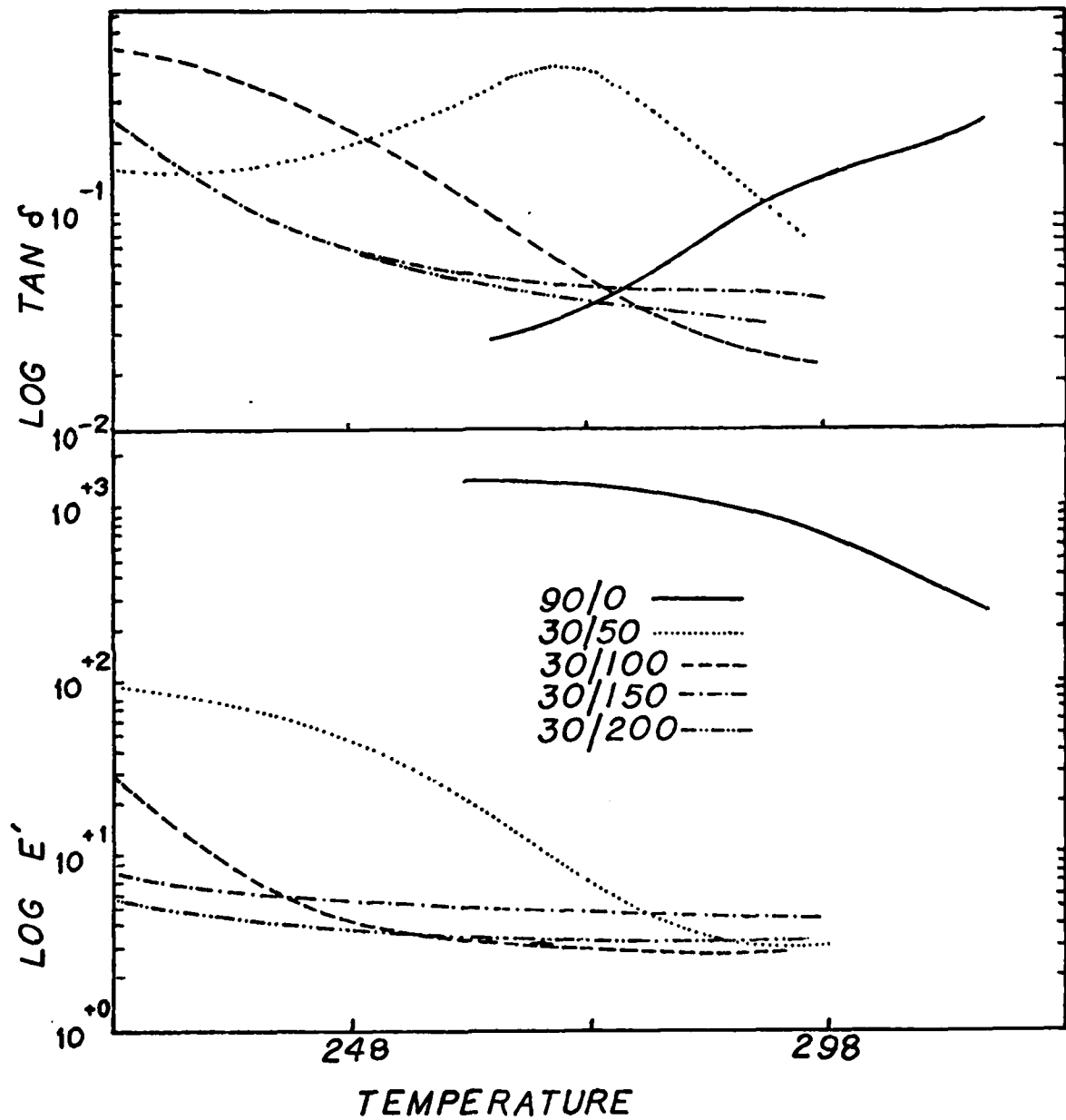


Figure 6: Dynamic mechanical properties of the diblocks and 1,2- PBD homopolymer previously treated with a 30MRad electron dose.

between crosslink junctions. Increased  $\log E'$  values in the rubbery region and shifts in the  $\tan \delta$  peaks towards higher temperatures are also apparent. These effects are well documented (18). Perhaps the most important result in Figure 6 is that the second maximum in  $\tan \delta$  for the (30/50) diblock sample is still present while the  $\tan \delta$  curves for the remaining diblocks no longer show the upward trends near  $0^\circ\text{C}$ . This curve flattening is also accompanied by a factor of two decrease in the magnitude of  $\tan \delta$ . Mackawa and Ferry (19) observed a similar decrease in the magnitude of  $\tan \delta$  in the rubbery zone increasing crosslink density. It was also shown that lightly crosslinked rubbers with higher initial molecular weight before crosslinking exhibited smaller mechanical losses than their lower molecular weight counterparts. It is interesting to note that the values of  $\log \tan \delta$  at  $20^\circ\text{C}$  for 2MRad samples (except (90/0)) in Figure 5 order themselves according to initial molecular weight. These results suggest that the same secondary loss mechanism reported by Ferry (who associated these losses with entanglement slippage) may be responsible for the increasing values of  $\tan \delta$  in the 2MRad samples. Higher crosslink densities were successful in eliminating this effect and eliminated the possibility of a second maximum in  $\log \tan \delta$  for the higher molecular weight diblocks near  $0^\circ\text{C}$ . The  $\tan \delta$  peak locations associated solely with the glass transitions of distinct phases and not caused by secondary losses are plotted as a function of composition in Figure 7 for the 2MRad samples. Included in this plot are the predicted positions of the  $\tan \delta$  peak for a random copolymer or miscible blend of 1,2- and 1,4- PBD based on the Fox equation. The error bars for these values of  $T_g$  are representative of the relative width of the damping peaks and correspond to those values of  $\log (\tan \delta)$  within 10% of the measured maxima.

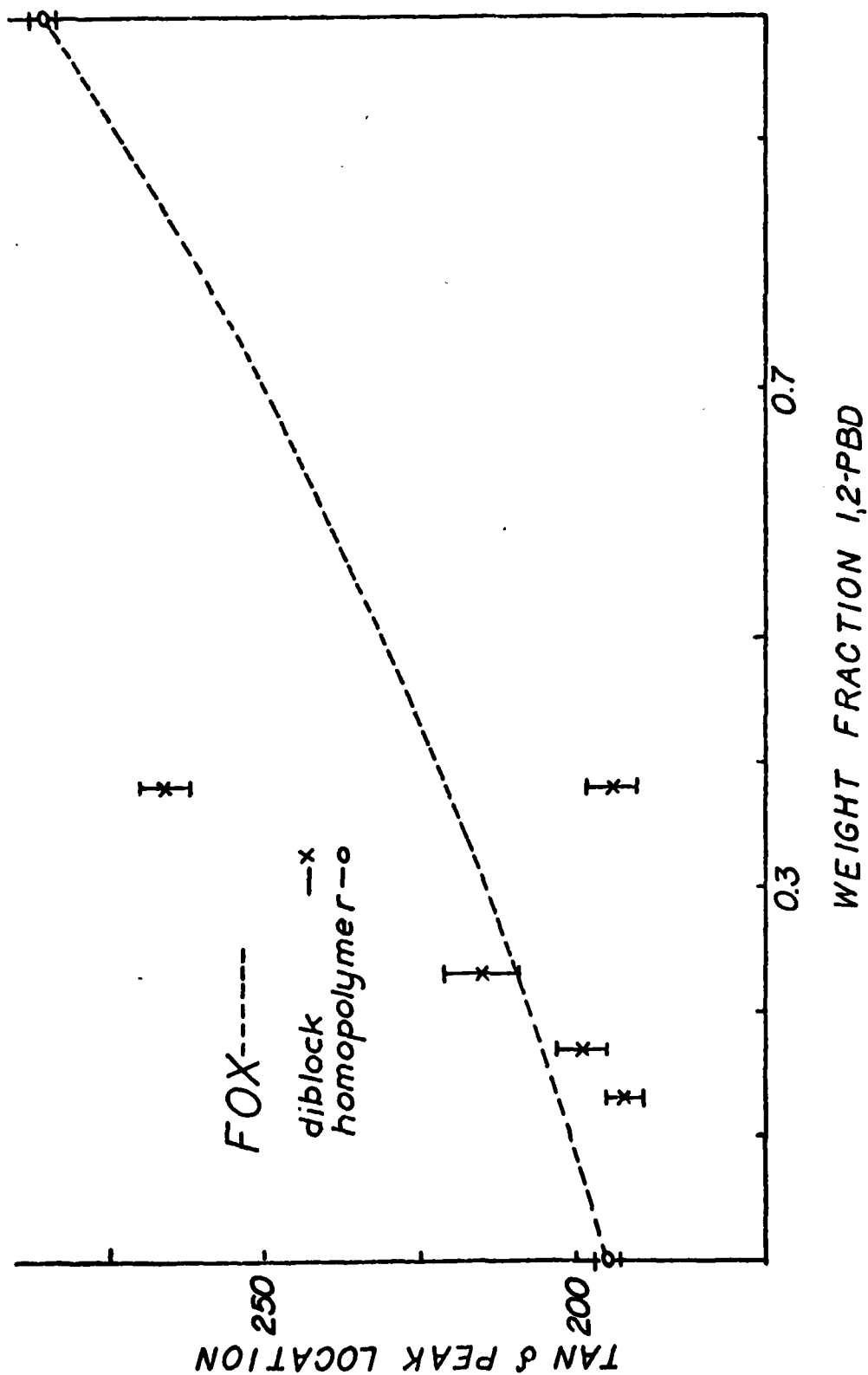


Figure 7: Tan  $\delta$  peak location vs. composition for diblocks and homopolymers crosslinked at 2MRad.

Unlike the earlier results from the DSC analysis, a clear distinction can be made between the heterogeneous character of the (30/50) sample and the homogeneity of the remaining diblocks. The better resolving power of dynamic mechanical testing in comparison to calorimetry has been reported by others (20). Here it was suggested that the molecular processes responsible for the observed changes in heat capacity detected by the DSC may involve longer range segmental motions than those responsible for dynamic mechanical loss peaks. The better resolution of the Rheovibron does illustrate that compatibility is operationally defined and that a given type of experiment will indicate compatibility or incompatibility depending upon the size of the molecular process it measures and the dimensions of possible phase domains.

Finally, the dynamic mechanical properties of 38% and 80% 1,2- PBD blends are shown with the parent PBD homopolymer in Figure 8. The results for these highly cross-linked samples (30MRad) are similar to those obtained for heterogeneous blends of polyisoprene and polybutadiene over the temperature range described by their homopolymer glass transitions (3-6). The log  $E'$  curves indicate that a change in the continuous phase from 1,4- to 1,2- PBD occurs between 38% and 80% 1,2- PBD.

#### Electron Microscopy

Representative transmission electron micrographs for the ebomite treated 1,2- and 1,4- PBD homopolymers are shown in Figure 9. These micrographs serve as a useful reference

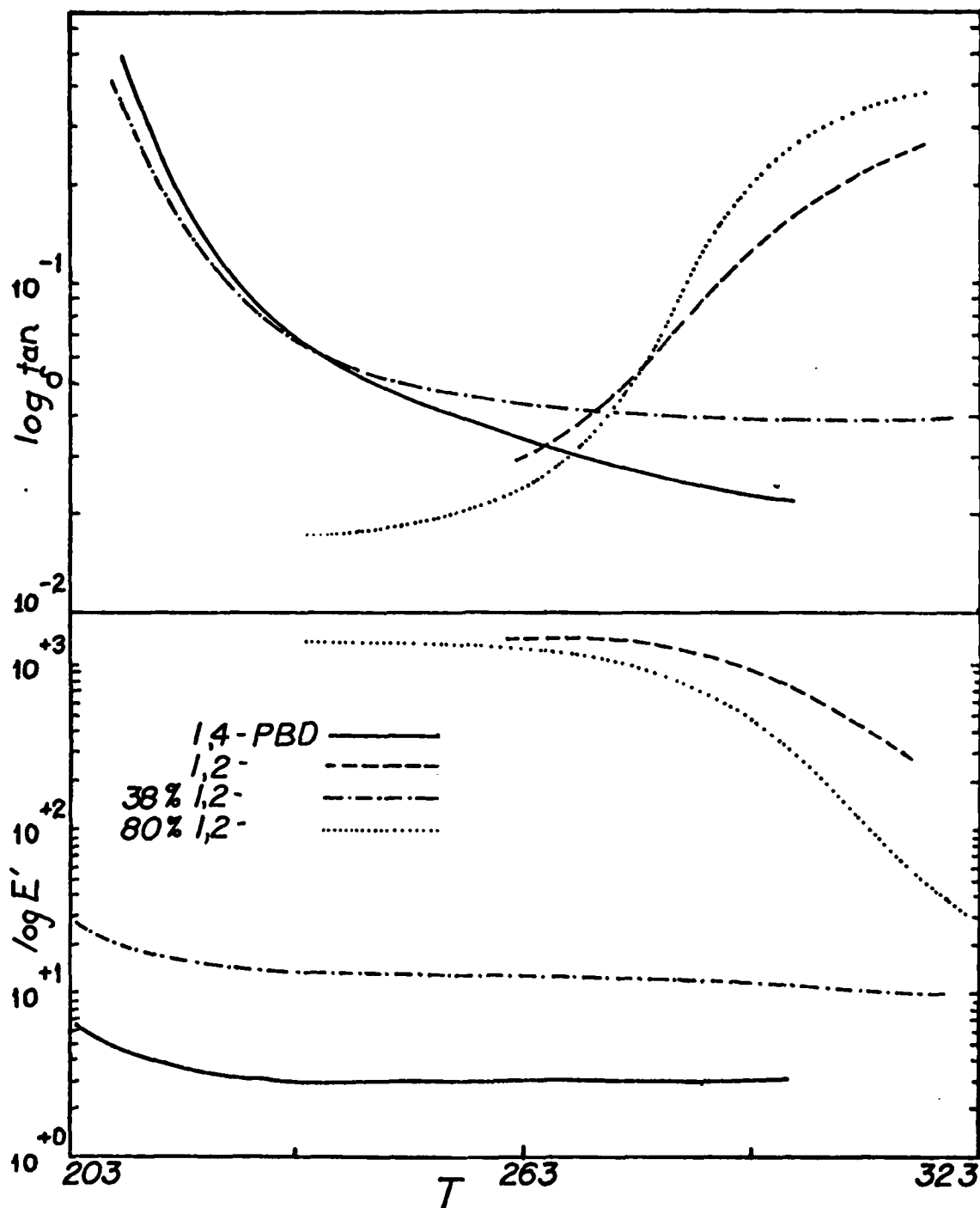


Figure 9: Dynamic mechanical properties of PBD homopolymers and homopolymer blends treated prior to testing with a 30MRad electron dose.

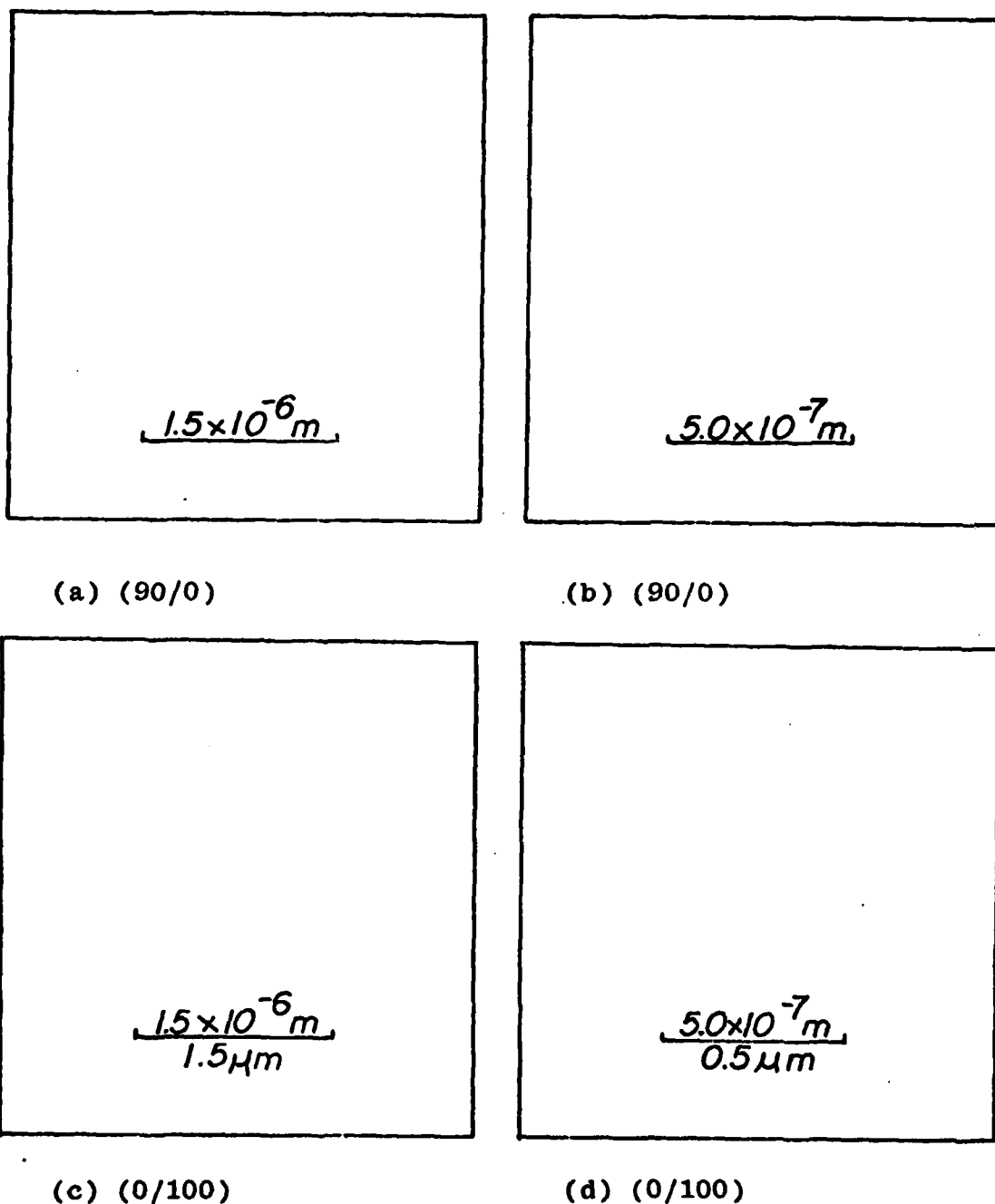
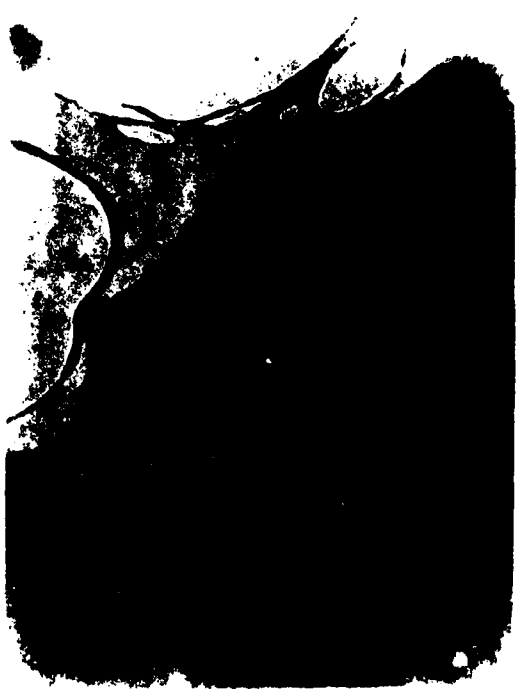
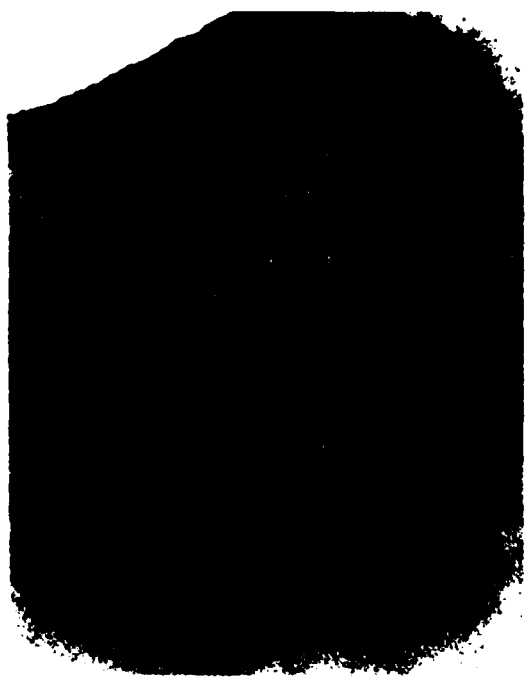


Figure 9: Transmission electron micrographs for the 1,2- and 1,4- PBD homopolymers. Sections (a) and (b) correspond to the 1,2- while (c) and (d) to the 1,4- PBD. Magnification as indicated.





when interpreting the forthcoming results for the various blends and diblock samples since the observable features in Figure 9 are certainly artifacts of the TEM technique. These extraneous features include a "salt and pepper" appearance in the 1,2- PBD micrographs which is commonly observed in homogeneous materials which have been subjected to heavy atom staining and microtome knife marks which appear as widely spaced parallel lines.

In each of the micrographs presented in Figure 9 and in subsequent figures, a hole or edge is included which can be used to judge the quality of the image. The intensity of the Fresnel fringes (the heavy white or black lines which border the edges of each opening) indicate the degree to which improper focusing of the electron beam may be generating false phase contrast. The degree of defocus necessary to generate this false phase contrast is inversely related to the magnification which means that visually distinct heterogeneity at relatively low magnification is conclusive evidence for phase separation. A good example of this type of conclusive evidence is given by Figure 10 which presents some micrographs for the homopolymer blends containing 12%, 38%, and 80% 1,2- PBD. These results acknowledge the incompatibility of the 1,2- and 1,4- PBD homopolymers in spin cast films which was observed in previous thermomechanical test results. It also illustrates the success of the ebonite method in differentiating between the 1,2- and 1,4- phases. Starting at the top of Figure 15, it appears that the dark, continuous matrix exists in samples with a high 1,4- PBD content indicating that the 1,4- phase has a higher concentration of sulfur. As in the dynamic mechanical property results, a phase inversion occurs at a composition somewhere between 38% and 80% 1,2- PBD which explains why the dark-stained 1,4- PBD has become the included phase as we move down the

(a) 12% 1,2- PBD

$$\frac{1.0 \times 10^5 m}{10 \mu m}$$

$$\frac{1.0 \times 10^5 m}{10 \mu m}$$

(b) 38% 1,2- PBD

$$\frac{1.0 \times 10^5 m}{10 \mu m}$$

(c) 80% 1,2- PBD

Figure 10: Micrographs for various blends of the 1,2- and 1,4- homopolymers. Magnification and wt.% as indicated.

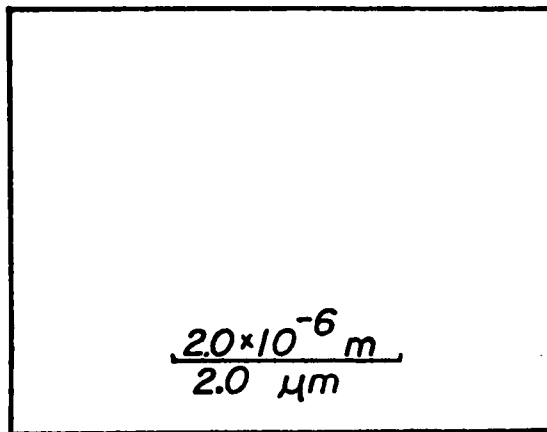


figure to the 80% blend. The size of the spherical inclusions in all of the blend micrographs varied from  $1 \times 10^3$  to  $5 \times 10^4$  nm (1 to 50  $\mu$ m) and appeared to be independent of composition. All of the cast films of these blends were transparent (which is a rather unique result for blends containing particles of this size) due to virtually identical refractive indices for each of the optically transparent homopolymer components (21).

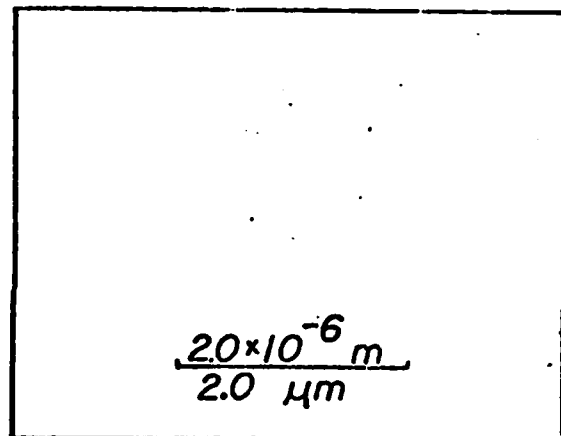
The last two figures contain representative electron micrographs for each of the four diblock copolymers which had been spin cast, crosslinked with a 30MRad electron dose, and ebonite treated prior to microtoming. Figure 11 shows sample slices of the (30/50), (30/100), and (30/200) diblocks magnified by  $\sim 12,000\times$ . At this magnification, the (30/50) sample consistently showed a fingerprint-like structure indicative of lamellar phase domains. The remaining diblocks, however, appeared homogeneous. The lamellar morphology of the 38% 1,2- PBD (30/50) diblock is drastically different than that of the corresponding blend from Figure 15 in terms of domain size as well as geometry. It is also interesting to compare the results for the (30/200) diblock to those of the blend which has a similar 12% 1,2- PBD content. While the blend is clearly heterogeneous the diblock is not suggesting a different morphology dependence on composition for these diblocks and blends. Figure 12 presents micrographs for each of the diblocks at a higher magnification. Again the (30/50) diblock exhibits separated phases organized into lamella whose width is  $\sim 20$  to 30 nm while the remaining diblocks appear homogeneous.

The

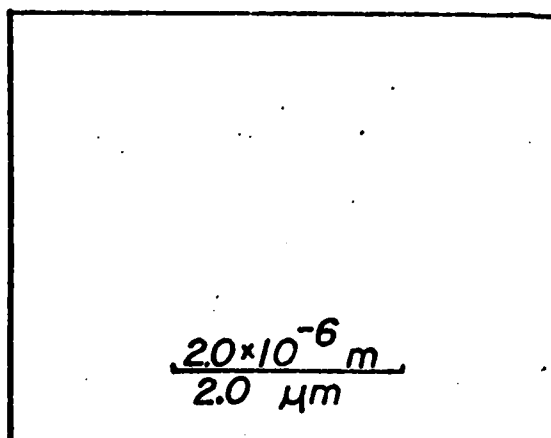
lamella boundaries in Figure 12 now seem less distinct than



(a) (30/200)

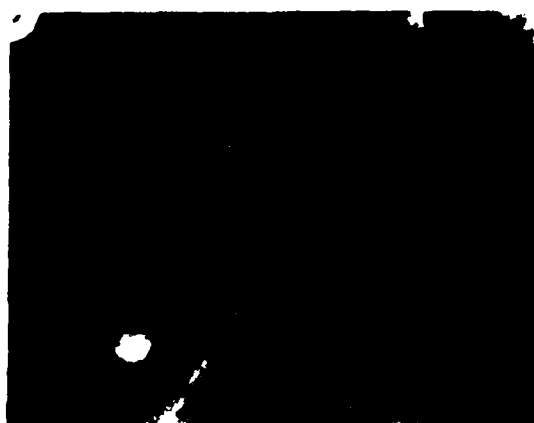
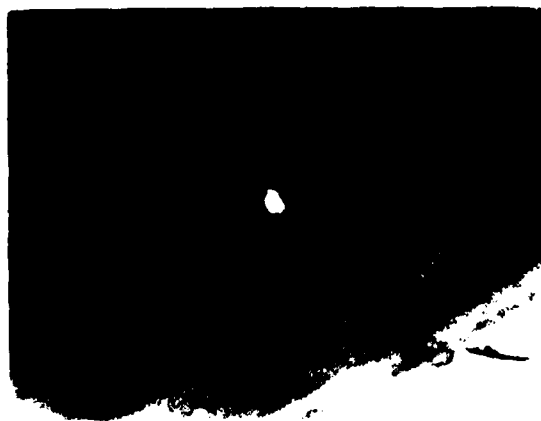


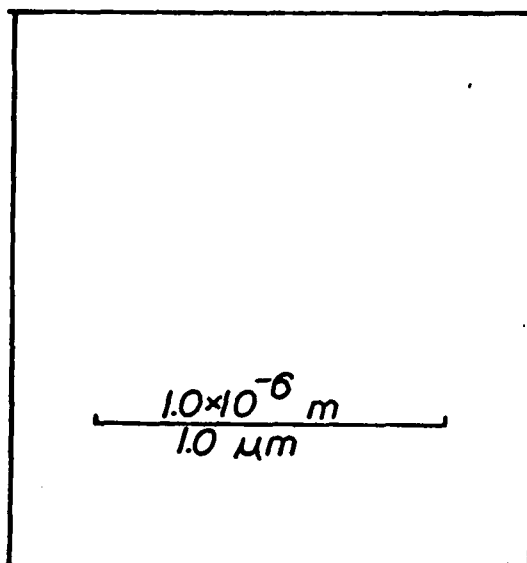
(b) 30/100)



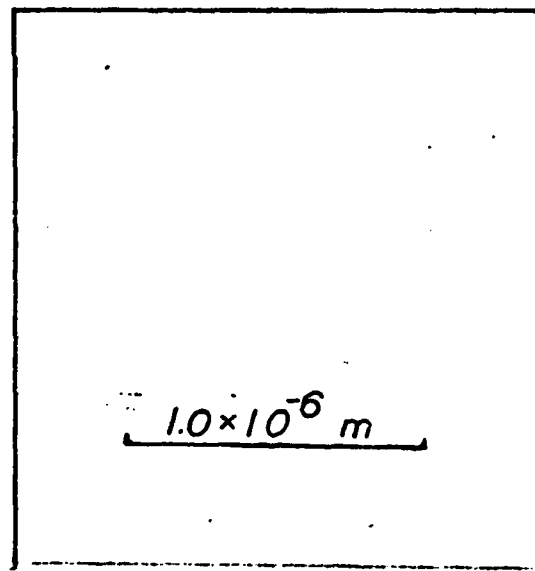
(c) (30/50)

Figure 11: Medium magnification micrographs for some of the diblock samples.

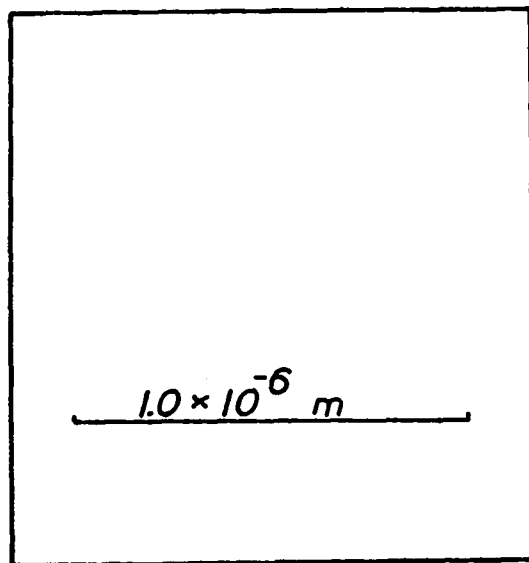




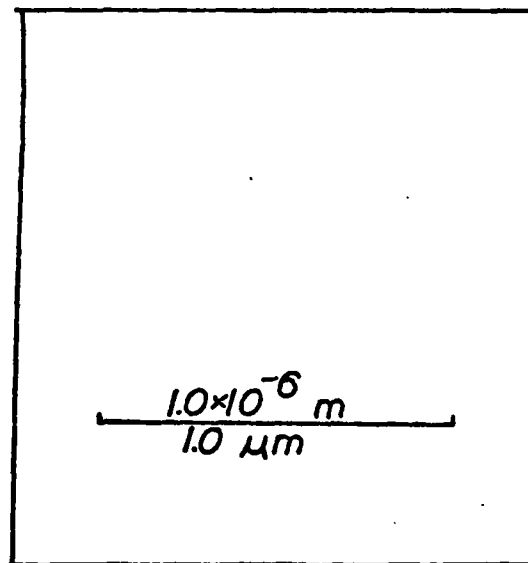
(a) (30/50)



(b) (30/100)



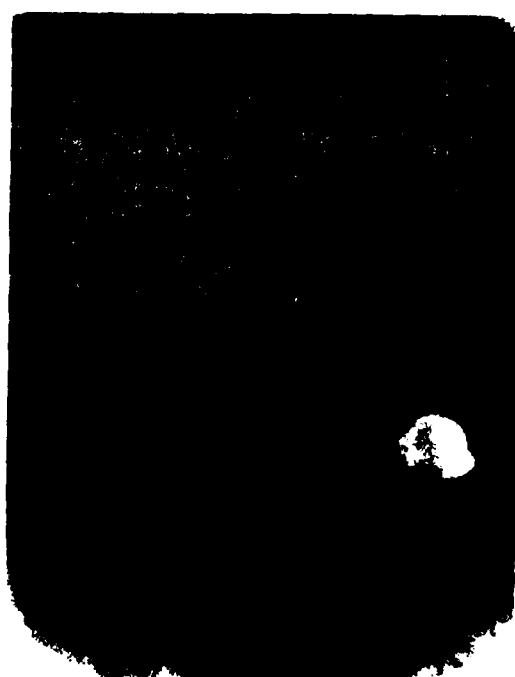
(c) (30/150)



(d) (30/200)

Figure 12: Higher magnification micrographs for the diblock copolymers.





one would expect based on the results obtained at the lower magnification. This could be due to a number of possibilities which include the sample thickness being considerably greater than the estimated domain width, the inability of the sulfur stain to clearly differentiate between each of the phases on such a small scale, or the existence of a diffuse phase boundary due to interfacial mixing.

As a final note, samples crosslinked with 2MRad electron doses prior to staining were also examined to see what effects the high temperature ebonite process (120°C) may have had on sample morphology. Although higher contrast resulted between phases in the 38% blend with no noticeable effect on morphology, the (30/50) samples provided no conclusive proof for the existence of distinct phases. This result may have been caused by an increased number of available vulcanization sites, i.e., greater sulfur staining, which in turn increased the apparent thickness of each microtomed specimen. Another possible cause for the absence of observable heterogeneity may be a result of the relaxed network constraints in these samples, due to lighter crosslinking, which could have allowed the (30/50) diblock to reequilibrate into a homogeneous form. Future tests on the dynamic shear storage modulus of these samples as a function of temperature should provide an accurate estimate of the homogenization temperature for the (30/50) diblock. These experiments should provide some valuable clues as to why the micrographs for the lightly crosslinked (30/50) diblock were ambiguous.

#### Mechanical Properties

Most of the previous mechanical property studies on rubbery block copolymers have focused on the commercially important triblock systems composed of a rubber center

block separating two glassy terminal segments. The higher percentage of rubber results in an elastomeric matrix which behaves like a crosslinked network. This is caused by the phase separation of the glassy terminal blocks into included domains which anchor both ends of each polymer chain. Not only do the polymers of this study lack the three segments necessary for the formation of a crosslinked rubber, but both components are above their glass transitions at room temperature. These materials act more like uncrosslinked elastomers by exhibiting cheesy behavior with low strength and elongation in the lower molecular weight samples and low strength but high elongations to break in the higher molecular weight specimens. This is shown in Figure 13 for some representative  $\sigma/\epsilon$  curves for uncrosslinked samples cast from toluene: samples were generally difficult to handle and the tests results were difficult to reproduce.

To generate materials with primarily elastic rather than viscous behavior, it was necessary to irradiate each sample with a beam of electrons. The chemical effects of bombarding the sample with high energy electrons are first the ionization of a polymer segment by the ejection of an electron followed by the dissociation of the cation to form a radical. From this point, the reaction is similar to peroxide crosslinking in that the polymer chain radicals formed couple to form tetrafunctional junctions (22). Figure 14 shows the stress-strain properties of the (30/100) diblock as a function of electron dose. A decreased value of  $M_c$  corresponding to an increased electron dose result in a higher value of stress at a given elongation.

The decrease in  $\epsilon_b$  with increased crosslinking is also in agreement with theoretical predictions of Taylor (23) which are based on studies of the ultimate properties of vulcanized rubbers.

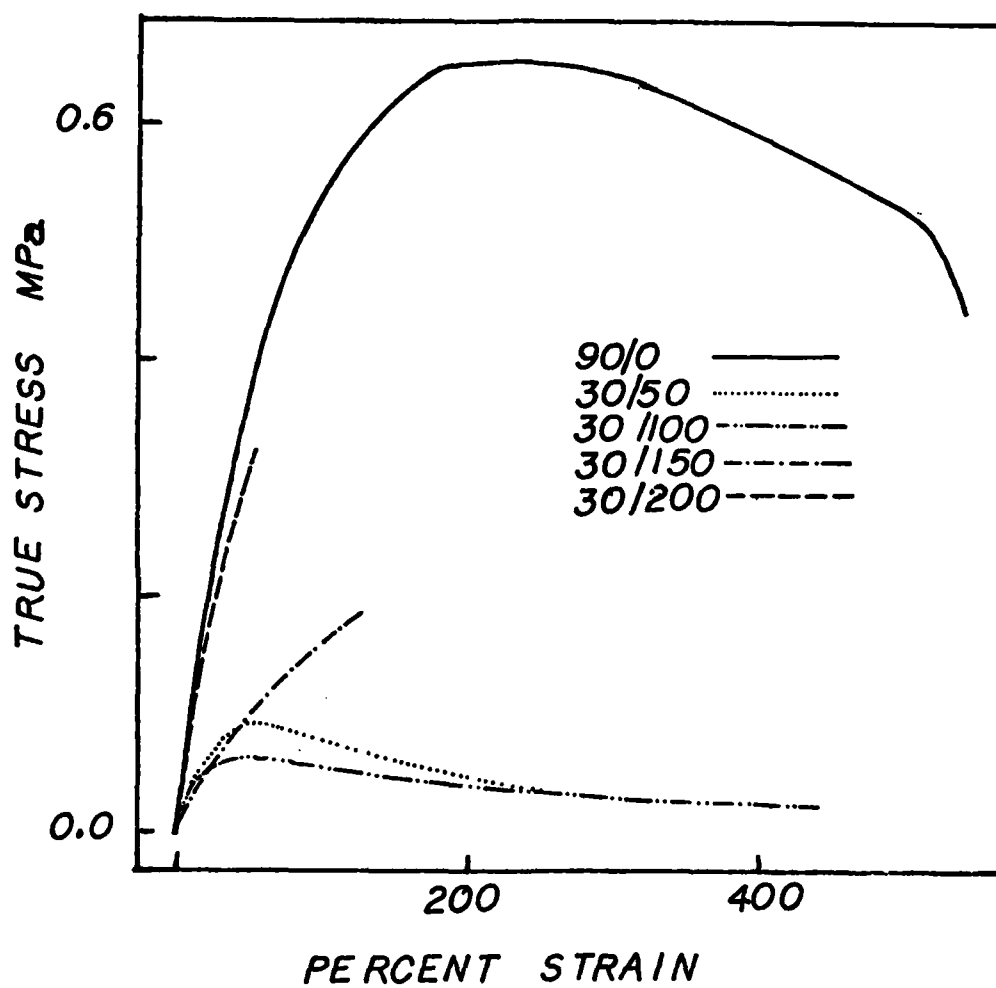


Figure 13: Representative stress-strain curves for the uncrosslinked diblocks and homopolymers spin cast from toluene.

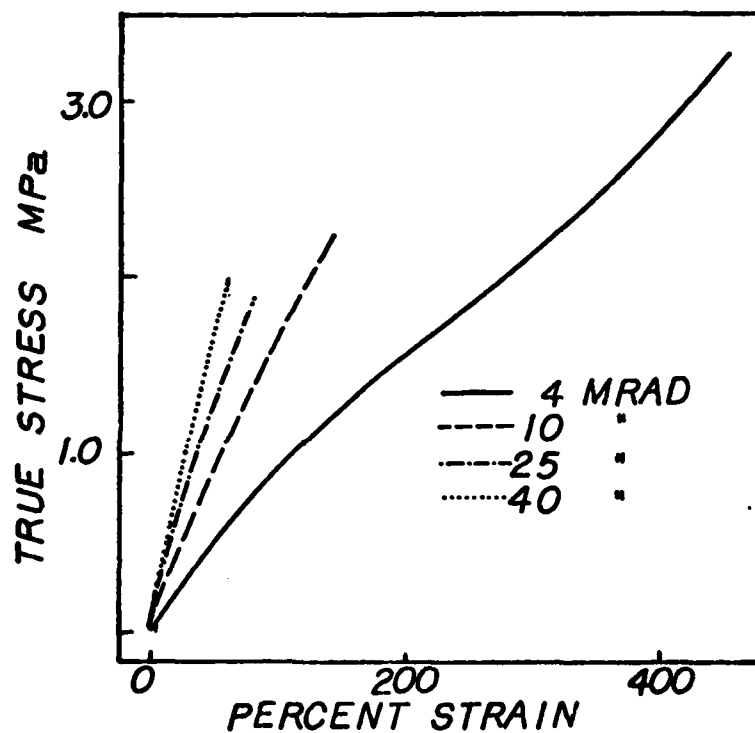


Figure 14. Tensile properties of the (30/100) diblock as a function of irradiation period. Various electron doses shown in MRad with corresponding stress-strain curve.

The tensile properties of block copolymers prepared by solvent evaporation generally show a dependence on the type of solvent from which the sample was cast. Seguela determined that systematic changes in microdomain structure due to differences in solvent affinity resulted in major changes in the tensile behavior of a series of polydiene-hydrogenated PS/PBD or PI/PS triblocks (15). In this case, decreasing solvent affinity for the PS phase resulted in high modulus specimens with lamellar microdomains being progressively transferred into lower strength cylindrical and spherical geometries. Another instance of solvent dependent tensile properties was observed in this lab for diblock samples of polystyrene and poly-1-butene (24). Samples spin cast from solvents which were good for both phases showed higher modulus and stress at break with decreased values of  $\epsilon_b$ . In this case, the change in tensile properties was attributed to better mixing between phases since the percentage of PS was so low (16% and 10% by weight) that only a spherical domain geometry was likely to exist. The stress-strain properties of three 1,2-PBD/1,4-PBD diblocks cast from cyclohexane and toluene are shown in Figure 15. The data indicate that the (30/50) diblock is significantly affected by casting solvent whereas the remaining diblocks are not. Previous results from the thermomechanical and electron microscopic analyses on the diblocks indicate that the (30/100) and (30/150) samples are homogeneous. This would explain the lack of solvent dependence in these materials while the heterogeneity of the (30/50) diblock provides a basis for the observed result. Based on the conclusions of Torradas (24), one would expect that the increase in modulus and decrease in  $\epsilon_b$  for the (30/50) diblock cast from toluene in comparison to that cast from  $C_6H_{12}$  means that toluene is a better solvent. This hypothesis

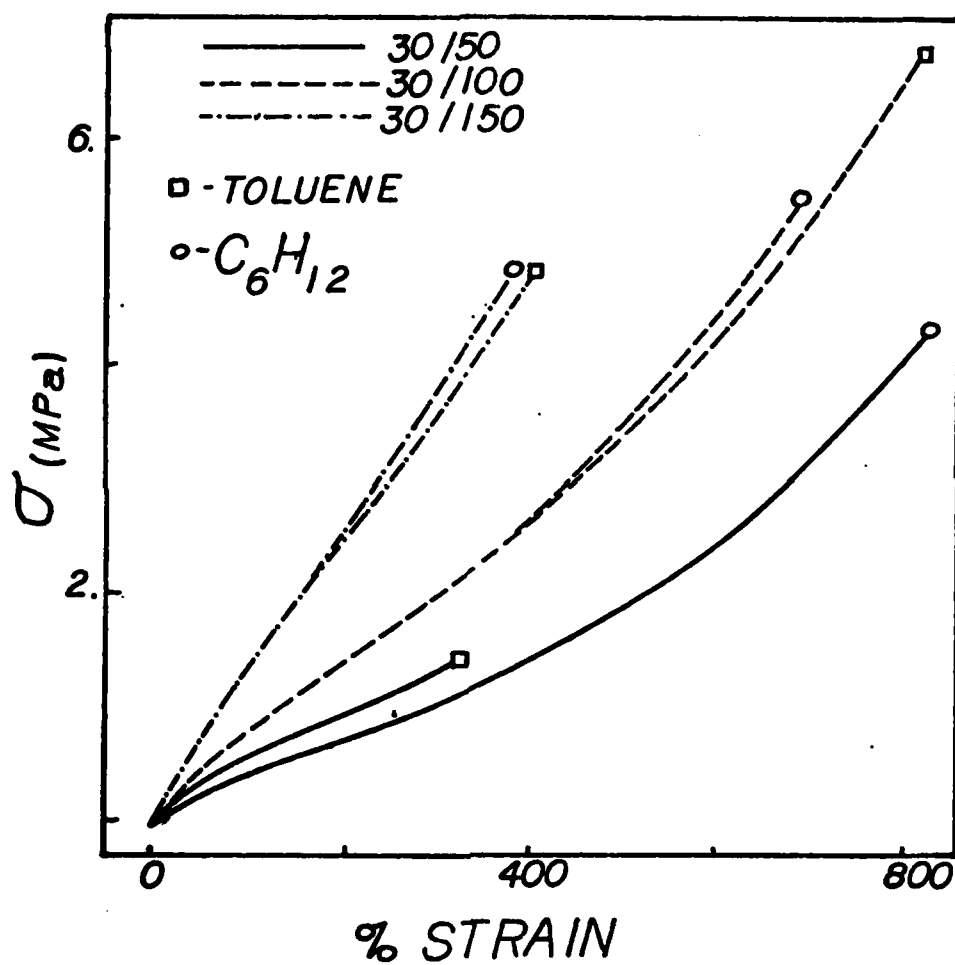


Figure 15: Tensile properties for various diblocks as a function of spin cast solvent.

was confirmed using swelling experiments which gave ( $V_f/V_o$ ) values of  $5.89 \pm 0.10$  with  $C_6H_{12}$  as a swelling solvent and  $6.26 \pm 0.03$  with toluene for (30/50) samples treated with a 10MRad electron dose prior to swelling.

It was stated earlier that the proximity to  $T_g$  and variation in crosslinking susceptibility may both have significant effects when comparing the tensile behavior of materials with differing chemical structure. Bovey reports (8) that the 1,2- repeat unit of polybutadiene is 1.7x more susceptible to radiation induced crosslinking than the 1,4-. It is also apparent from previous thermal property data that the 1,2- PBD homopolymer is also much closer to  $T_g$  at room temperature. With this in mind, the stress-strain curves for the diblock and parent homopolymers crosslinked with a 4MRad electron dose are presented in Figure 16. These show the 1,2- PBD exhibiting the expected lower extensibility and higher modulus and stress-at-break value than the 1,4- PBD. The stress-strain curves of the diblocks, however, do not show increased modulus and decreased extensibility corresponding to increased 1,2- PBD content. It is also interesting to note that the (30/50) and (30/200) samples lie outside the stress-strain envelop described by the parent homopolymers. The ordering of the diblock stress-strain curves in Figure 16 does suggest that a dependence on sample molecular weight  $\bar{M}_n$  prior to crosslinking may exist (25).



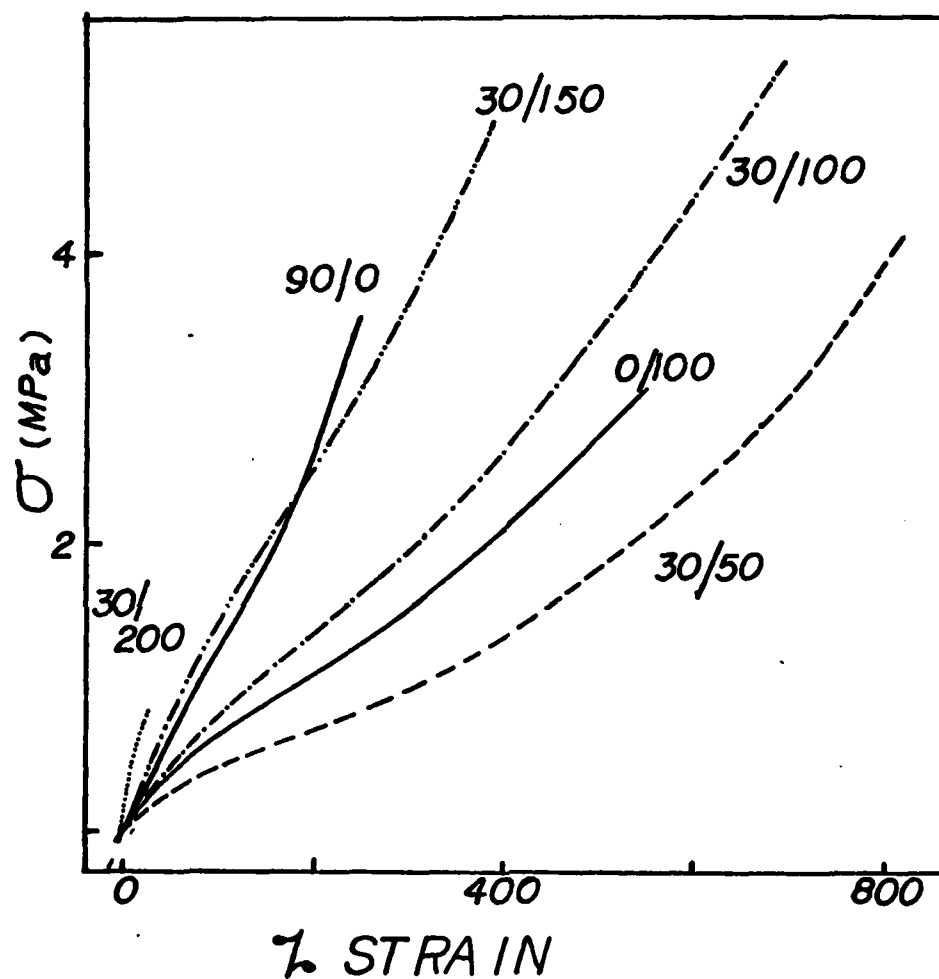


Figure 16: Representative stress-strain curves for the diblocks and homopolymers spin cast from cyclohexane and treated with a 4MRad electron dose.

To assess the extent of the variation of  $M_c$  with composition and thereby provide additional insight into its possible contribution to the primary molecular weight dependent tensile properties of the lightly crosslinked diblocks, swelling experiments were conducted on diblocks exposed to a 10MRad electron dose.  $V_f/V_o$  versus %1,4- PBD block values are shown in Figure 17 for the diblocks, parent homopolymers, and various homopolymer blends swollen in cumene  $C_6H_5CH(CH_3)_2$  at room temperature. The degree of swelling exhibited by the diblocks and homopolymers correlates well with the tensile properties of these samples shown in Figure 16.

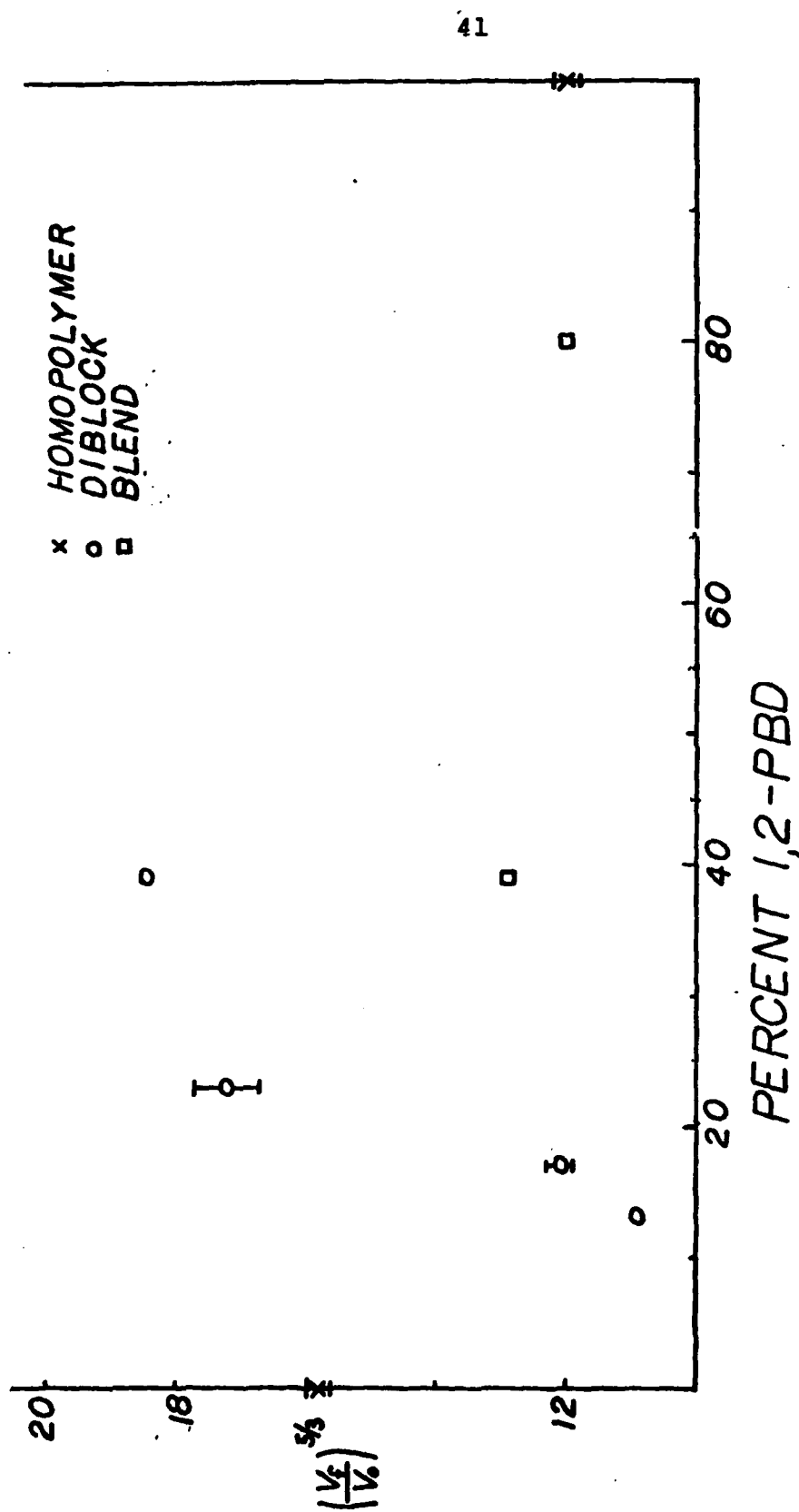


Figure 17: Equilibrium swelling ratio vs. composition for the diblocks, homopolymers, and homopolymer blends treated with a 10MRad electron dose prior to swelling in cumene.

Figure 17 also indicates that the homopolymer blends, which have a virtually constant molecular weight with varying composition, show a linear variation in swelling ratio with 1,4- PBD content. The (30/50) diblock, however, whose overall molecular weight and composition are very similar to that of the 62% 1,4- PBD homopolymer blend, exhibits a much greater degree of swelling. This suggests that morphological differences in otherwise identical samples may have significant effects on the degree of crosslinking. Finally, the differences between sample swelling ratios  $\Delta(V_f/V_o)$  in Figure 17 are considerably less than those observed in the case of a 4MRad dose. This illustrates the rapid diminuation of primary molecular weight effects with decreasing  $M_c$ .

In an attempt to eliminate the dependence of the tensile properties on the initial molecular weight, diblocks, homopolymers, and two homopolymer blends were heavily crosslinked with a 30MRad electron dose prior to mechanical testing. The stress-strain results for the homopolymers and blends are shown in Figure 18. The difference in modulus between the two homopolymers has increased dramatically in comparison to the results from the 4MRad sample tests. This is due to the  $1/M_c$  dependence of stress and to the shift in  $T_g$  for the 1,2- PBD caused by the higher crosslinking. Figure 18 also shows a regular increase in modulus corresponding to increased 1,2- PBD content for the homopolymer blends. This behavior is probably the result of a corresponding decrease in  $M_c$  with increased 1,2- content which was noted earlier in the results from the swelling studies.

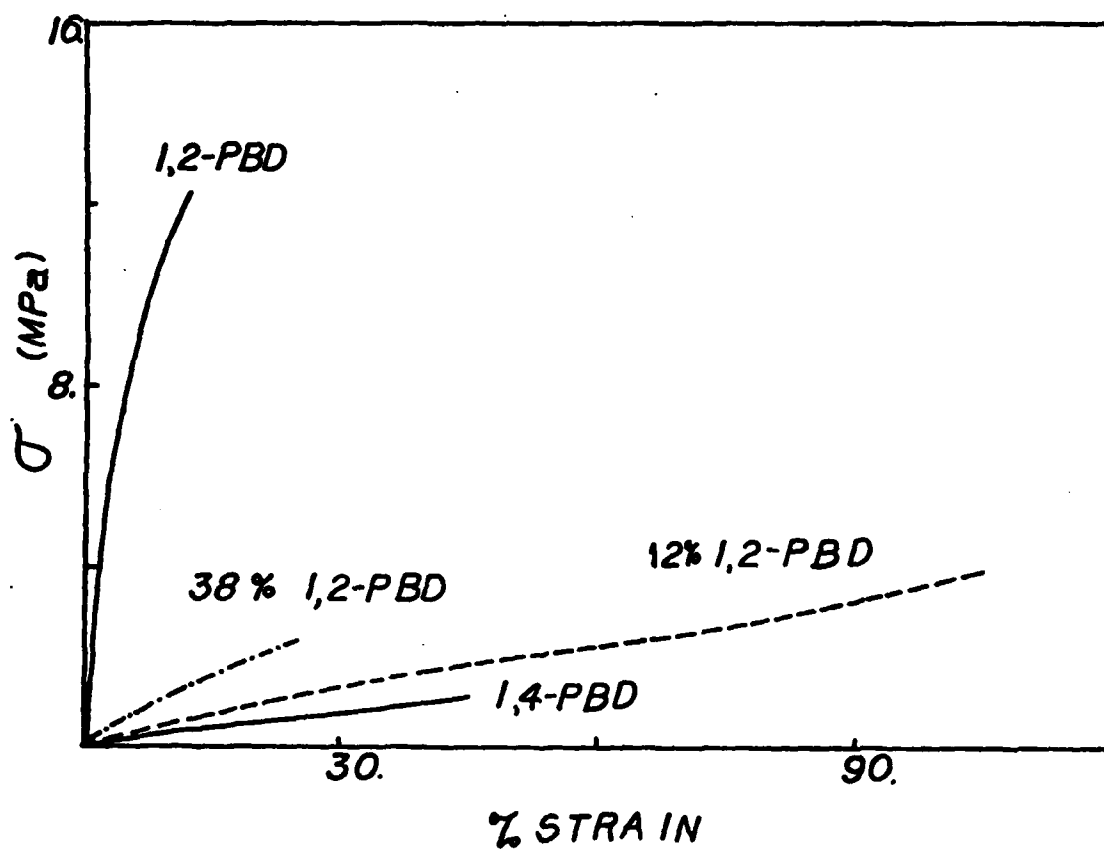


Figure 18: Stress-strain results for the PBD homopolymers and their blends treated prior to testing with a 30MRad electron dose.

The stress-strain curves for the more heavily crosslinked diblocks and the 1,4- PBD homopolymer are shown in Figure 19. Unlike the results for the corresponding blends, these curves indicate that there is no significant differences in the tensile properties between the diblocks and 1,4- homopolymer inspite of their differences in composition. Although the modulus for the 12% 1,2- PBD blend and the corresponding (30/200) diblock were virtually identical, the strain-at-break for the heterogeneous blend was nearly twice that of the diblock.

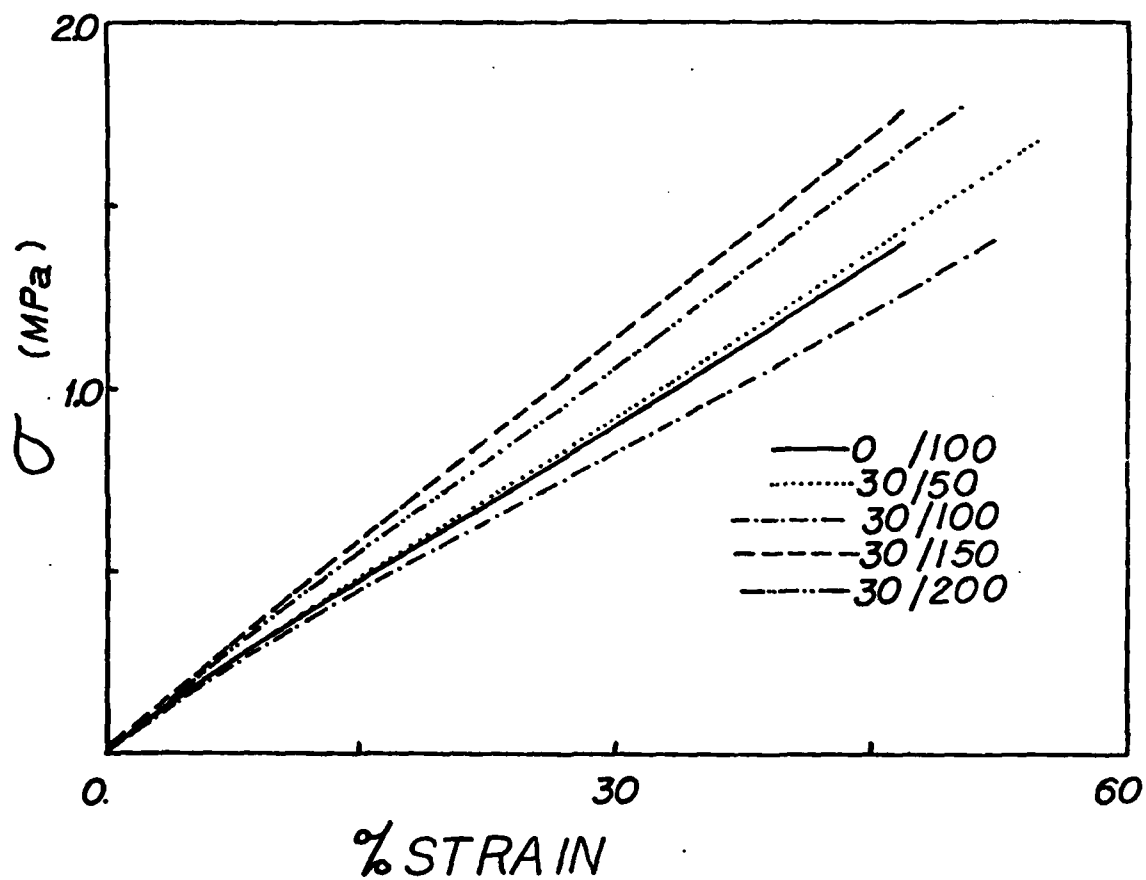


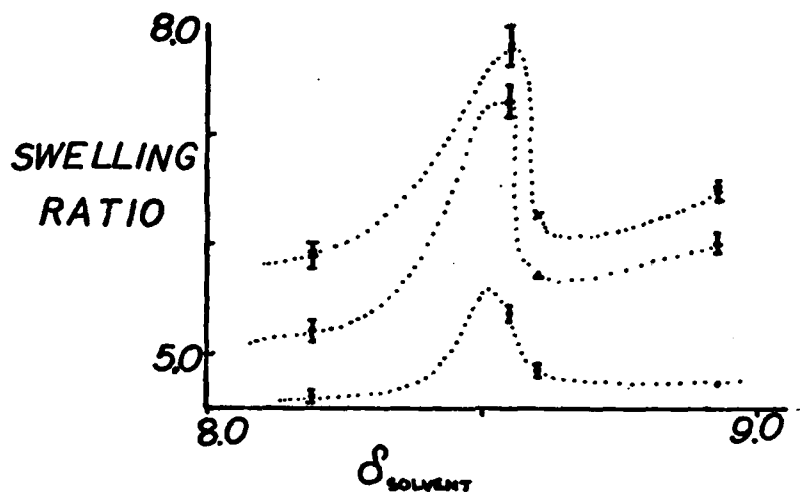
Figure 19: Representative stress-strain curves for the 1,4- PBD homopolymer and the various diblocks treated with a 30MRad electron dose.

The equilibrium swelling ratios for the two homopolymers and the (30/50) diblock crosslinked prior to swelling with a 10MRad electron dose were measured as a function of solvent affinity in an attempt to establish more accurate estimates of solubility parameter  $\delta$  than those listed in the literature for 1,2- and 1,4- PBD. A similar plot was used by Samuels and Wilkes (25) to determine the number of phases in a crosslinked PS/PBD block copolymer by measuring the number of maxima in the swelling curve. Figure 20 shows the resulting ( $V_f/V_o$ ) values for polymers of this study as a function of tabulated swelling solvent solubility parameter (from Hoy and Brandrup and Immergut (27,21)). Unlike the results of Samuels, the differences in  $\delta_{1,2-}$  PBD and  $\delta_{1,4-}$  PBD were so slight that only one maximum was apparent in the swelling curve of the heterogeneous (30/50) diblock. The calculated  $\delta$  values for the 1,2- and 1,4- PBD homopolymers using the group contribution techniques of Small and Hoy (28) are shown tabulated on the next page with the experimental values based on the  $\delta_{\text{solvent}}$  values of Brandrup (21).

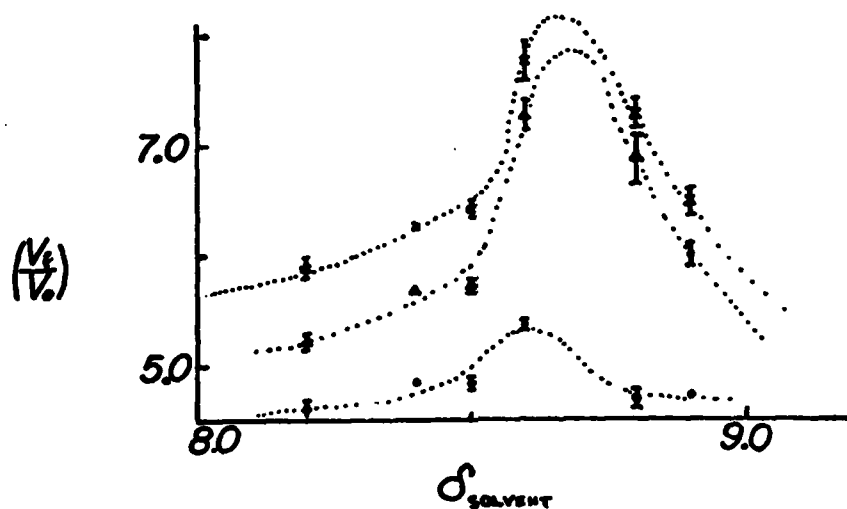


<u>Sample</u>	<u><math>\delta_{\text{Small}}</math></u>	<u><math>\delta_{\text{Hoy}}</math></u>	<u><math>\delta_{\text{experimental}}</math></u>
1,4- PBD	8.29	8.59	8.4-8.8
1,2- PBD	8.10	8.25	8.4-8.8

The data also suggest that despite the uncertainty in the solvent  $\delta$  values the difference in  $\delta$  for the two homopolymers is less than  $0.4 \text{ cal}^{\frac{1}{2}} \text{ cm}^{-\frac{1}{2}}$ .



(a) Hoy



(b) Immergut and Brandrup

Figure 20: Equilibrium swelling ratio vs.  $\delta_{\text{solvent}}$  for the (30/50) diblock and the parent homopolymers all treated with a 10MRad electron dose. Plots (a) and (b) are shown to illustrate the discrepancy in the tabulated values for  $\delta$ . The source of  $\delta_{\text{solvent}}$  for each plot is indicated.

## Conclusions

### Morphology Characterization

The results from the thermomechanical and transmission electron microscopy analyses gave clear evidence for the existence of two phases in the homopolymer blends of 99% 1,2- and medium cis 1,4- polybutadiene. This is in complete agreement with previous results of this lab (5) for blends of PBD of differing microstructure (65% 1,2- and medium cis 1,4-) which also exhibited heterogeneity. Spherical inclusions of the minor phase were observed, using electron microscopy, whose diamters were 1-50 microns in size. Despite the absence of two endotherms in our DSC traces of the (30/50) diblock spin cast from various solvents and with different thermal histories, the dynamic mechanical properties indicate distinct two-phase behavior. Additional support of the dynamic property results was provided by TEM studies which showed lamellar microdomains whose width varied from 20 to 30nm. The remaining diblocks of lower % 1,2- PBD but greater overall molecular weight were shown to be homogeneous in all of the tests performed.

The transition from hetero- to homogeneous morphologies in the diblock samples provides a useful means of testing some of the proposed thermodynamic theories. Figure 21 shows a phase diagram calculated for a diblock series of polystyrene and polybutadiene using Helfand's expression for the free energy of mixing (29). This particular diagram is used because all of the experimental values necessary for the direct application of this theory to the sample series of this project have not yet been determined. While the Kuhn parameters (29) used to calculate this curve are probably reasonable first estimates,

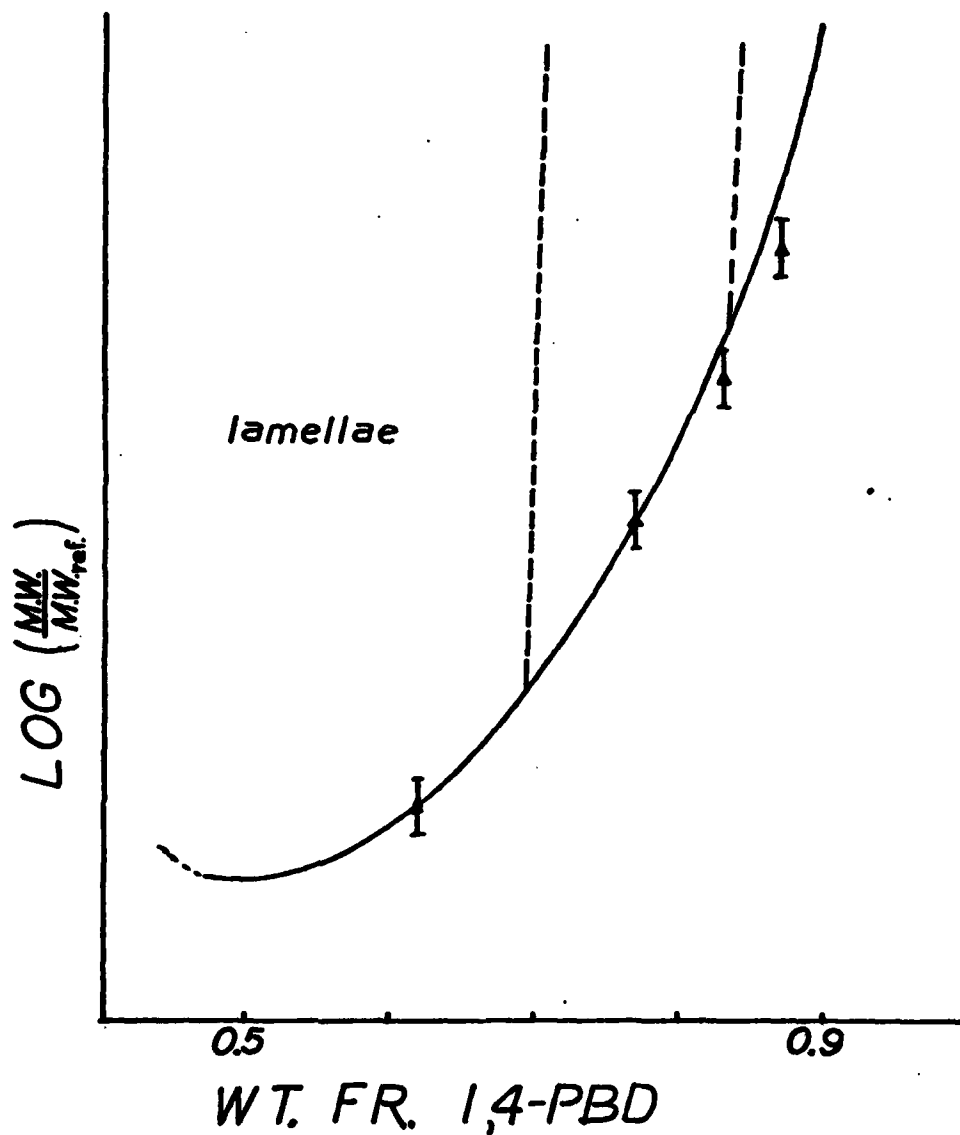


Figure 21: Phase diagram for a diblock of PS and PBD based on free energy calculations of Helfand. Also shown are the data for the samples of this study. The reference molecular weight is 74K.

the interaction parameter is not. It is assumed that shifting this phase transition curve vertically through the selection of a suitable reference molecular weight will circumvent the discrepancy in  $\chi$ . This reference molecular weight value was chosen so that the (30/50) diblock lies directly on the hetero-to homogeneous phase transition curve. The general trend of the plot fits the data remarkably well. The strong dependence on composition apparent in the theoretical curve seems to account for the homogeneous morphologies in the lower % 1,2- PBD (30/100), (30/150), and (30/200) diblocks.

Figure 27 shows the theoretical hetero-to homogeneous diblock transition curve predicted by Leibler (30). The illustrated phase transition curve is based on monodisperse polymer chains where each block has the same segment Kuhn statistical length. The terms  $N_A$  and  $N$  represent the number of repeat units of component A and the total number of repeat units per chain, respectively. The value for the segment interaction parameter  $\chi$  was estimated for the samples by setting the value of  $\chi N$  for the (30/50) diblock on the lamellar to cylindrical microdomain geometry transition within the heterogeneous region. This value of  $\chi N$  is in good agreement with the experimental estimate of  $\chi \sim 10$  determined from swelling results of Figure 25.

Unlike the previous figure, the sample values all fall within the heterogeneous region. Since the data points again follow the curve when going to lower 1,2- content, experimental inaccuracies in the values of molecular weight and composition combined with the equal Kuhn length assumption could easily account for this lack of agreement.

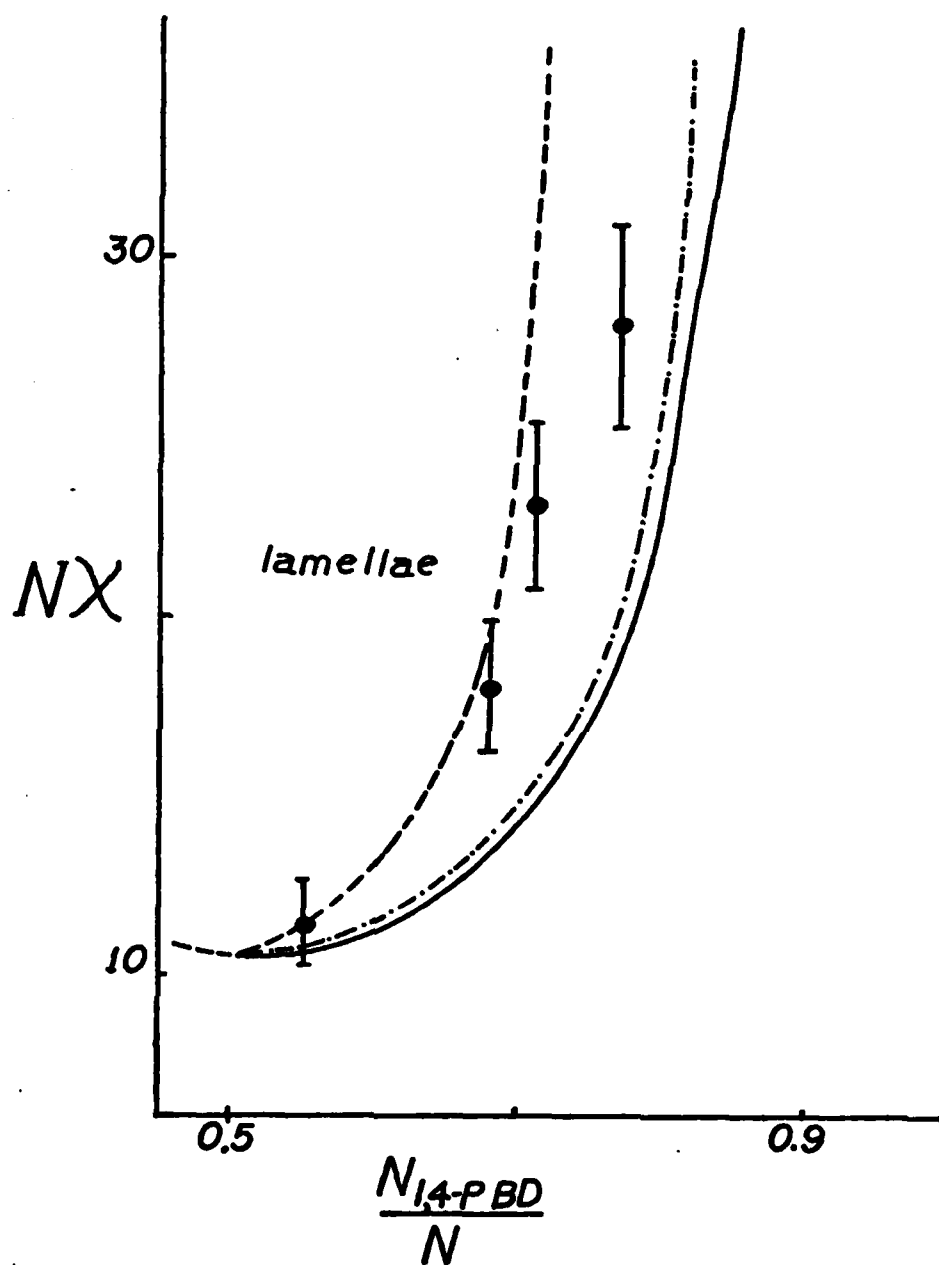


Figure 22: Generalized phase diagram of Leibler for a diblock copolymer indicating the homo-to heterogeneous phase transition and the most stable domain geometries as a function of composition.  $N_A$  and  $N$  represent the number of repeat units of component A and the total number of repeat units in the polymer chain.

### Mechanical Properties

In general, the tensile properties were strongly dependent on the initial sample molecular weights up to  $\beta$ -radiation doses of 30MRad. This dependence became less pronounced with increasing electron dose where the effects of compositional variation, manifested in varying  $M_c$  values, began to dominate stress-strain behavior. This type of behavior has been observed in other elastomers and is in agreement with the relationships developed in the statistical theory of rubber elasticity. The higher modulus and stress-at-break for the 1,2- PBD in relation to the 1,4-homopolymer was attributed to its higher crosslink density and closer proximity to  $T_g$ . Spherical phase domains in the homopolymer blends containing <50% 1,2- PBD served as reinforcing filler particles - modulus and stress-at-break values were increased over those of the 1,4- homopolymer. All of the homopolymer blends fell within the stress-strain envelop described by the 1,2- and 1,4- PBD samples. The microheterogeneous (30/50) diblock, however, exhibited distinctly different stress-strain curves than its corresponding homopolymer blend. Swelling studies suggested that the degree of mixing between phases has a considerable effect on the crosslinking process. The effective  $M_c$  values for the diblock are considerably greater which explains the lower modulus and stress-at-break.

## REFERENCES

1. A.F. Halasa, D.M. Schulz, C.P. Tate, and V.D. Mochel, Adv. in Organometallic Chem., 18, 55 (1980).
2. A.F. Halasa, personal communication, 10/23/79.
3. A.R. Ramos and R.E. Cohen, Polymer Eng. Sci., 17, 639 (1977).
4. R.E. Cohen and A.R. Ramos, Macromolecules, 12, 131 (1979).
5. R.E. Cohen and A.R. Ramos, Adv. Chem. Series, 176, 237 (1979).
6. R.E. Cohen and A.R. Ramos, J. Macromol. Sci. Phys., B17, 625 (1980).
7. D.H. Kaelble, J. Appl. Polym. Sci., 9, 1209 (1965).
8. F.A. Bovey, "The Effects of Ionizing Radiation on Natural and Synthetic High Polymers", Interscience Publishers, New York, 1958.
9. N. Ho-Duc and J. Prud'homme, Macromolecules, 6, 472 (1973).
10. D.J. Massa, J. Appl. Phys., 44, 2595 (1973).
11. A.R. Ramos, F.S. Bates, and R.E. Cohen, J. Polym. Sci. Phys. Ed., 16, 753 (1978).
12. A. Voet and J.C. Morawski, Rubber Chem. Technol., 47, 758 (1974).
13. R.W. Smith and J.C. Andries, Rubber Chem. Technol., 47, 64 (1974).
14. F.A. Bovey, "High Resolution NMR of Macromolecules", pp.224-225, Academic Press, New York, 1972.
15. R. Seguela and J. Prud'homme, Macromolecules, 5, 1007 (1978).
16. J.M. Cowie, D. Lath, and I.J. McEwen, Macromolecules, 12, 52 (1979).
17. O. Olabisi, L.M. Robeson, and M.T. Shaw, "Polymer-Polymer Miscibility", p. 279, Academic Press, New York, 1979.
18. L.E. Nielsen, "Mechanical Properties of Polymers and Composites", Vol. 1, pp. 9-10, Marcel Dekker, Inc., New York, 1974.



19. E. Maekawa, R.G. Mancke, and J.D. Ferry, J. Phys. Chem., 69, 2811 (1965).
20. J. Stoelting, F.E. Karasz, and W.J. MacKnight, Polym. Sci. Eng., 10, 133 (1970).
21. J. Brandrup and E.H. Immergut, "Polymer Handbook", 2nd ed., Wiley, New York, 1975.
22. G. Odian, "Principles of Polymerization", pp. 187, 621, McGraw-Hill, New York, 1970.
23. G.P. Taylor and S.P. Darin, J. Polym. Sci., 17, 511 (1955).
24. R.E. Cohen, J.M. Torradas, D.E. Wilfong, Polymer Preprints, 21(2), 216 (1980) and unpublished results.
25. D.E. Wilfong, S.M. Thesis, Massachusetts Institute of Technology, February, 1981.
26. S.L. Samuels and G.L. Wilkes, Polym. Eng. Sci., 13, 280 (1973).
27. K.L. Hoy, J. Paint Technol., 42, 76 (1970).
28. H. Ahmad and M. Yaseen, Polym. Eng. Sci., 19, 858 (1979).
29. E. Helfand and Z.R. Wasserman in "Developments in Block Copolymers", I. Goodman Ed., Applied Science Publishers Ltd., London, (to be published).
30. L. Leibler, Macromolecules, 13, 1602 (1980).